Title: Supramolecular attack particles are autonomous killing entities released from cytotoxic T-cells

Authors: Š. Balint[1], S. Müller[2], R. Fischer[3], B. M. Kessler[3], M. Harkiolaki[4], S. Valitutti[2,5] and M. L. Dustin[1*]

Affiliations:

1. Kennedy Institute of Rheumatology, Nuffield Department of Orthopedics, Rheumatology and Musculoskeletal Sciences, The University of Oxford, Oxford, UK

2. Cancer Research Center of Toulouse, INSERM, Toulouse, France

3. Discovery Proteomics Facility, Target Discovery Institute, Nuffield Department of Medicine, The University of Oxford, Oxford, UK

4. Diamond Light Source, Harwell Science and Innovation Campus, Chilton, Didcot, UK

5. Department of Pathology, Institut Universitaire du Cancer-Oncopole, Toulouse, France

*Corresponding author: michael.dustin@kennedy.ox.ac.uk

Abstract: Cytotoxic T lymphocytes (CTLs) kill infected and cancerous cells. We detected transfer of cytotoxic multiprotein complexes from CTLs to target cells, termed Supramolecular Attack Particles (SMAPs). SMAPs were rapidly released from CTLs and were autonomously cytotoxic. Mass spectrometry, immunochemical analysis and CRISPR editing identified a C-terminal fragment of thrombospondin-1 as an unexpected SMAP component that contributed to target killing. Direct stochastic optical reconstruction microscopy resolved a cytotoxic core surrounded by a thrombospondin-1 shell of ~120 nm diameter. Cryo-Soft X-ray Tomography analysis revealed that SMAPs had a carbon-dense shell and were stored in multicore granules. We propose that SMAPs are autonomous extracellular killing entities that deliver cytotoxic cargo based on specificity of shell components.

One Sentence Summary: Supramolecular attack particles with a dense shell and cytotoxic core are autonomous killing entities released from cytotoxic T-cells.

Main Text: Cytotoxic T lymphocytes (CTLs) exocytose soluble granzymes and perforin (Prf1) from secretory lysosomes (SLs) into the interface between the CTL and target cell, the cytotoxic immunological synapse (IS) (*1-5*). Prf1 forms pores in the plasma membrane of target cells that mediate entry of granzymes, such as granzyme B (Gzmb) into the target cell cytoplasm. Cytoplasmic Gzmb initiates multiple pathways leading to target cell death (*6-8*). Gzmb and Prf1 are stored inside SLs in condensates with serglycin (Srgn) (*9, 10*). There are reports that Prf1 and Gzmb may be released in particles (*11-13*), but their nature has remained elusive. To address this, we designed an experiment to follow putative cytotoxic particles from CMV pp65 specific human CTL clones (*14*) to target cells bearing pp65-HLA-A2 complexes. The CTL clones were transfected with mRNA encoding Gzmb-mCherry-SEpHluorin that concentrated in SLs. The SLs were also co-labeled with Alexa 647-wheat germ agglutinin (WGA) (*15*). WGA does not interact with high mannose oligosaccharides of Gzmb (*16, 17*) such that co-transfer of Gzmb and WGA to the target would implicate a multi-glycoprotein particle. The double-labeled CTLs were mixed with HLA-A2 positive target cells with or without the pp65 peptide and subjected to time-lapse microscopy. Within minutes of mixing, the pp65 pulsed targets contained intense double-positive puncta, whereas unpulsed target cells lacked these signals after interaction with the CTLs (Fig. 1A, Fig. S1 and Movie S1-3). We defined these multiprotein structures as supramolecular attack particles (SMAPs) and subjected them to further analysis.

We first investigated the kinetics of SMAPs release. We incubated Gzmb-mCherry-SEpHluorin transfected human $CD8^+$ T-cells on a supported lipid bilayers (SLB) coated with laterally mobile ICAM-1 and anti-CD3ε (Fig. 1B, Fig. S2) (*18*). Total internal reflection fluorescence microscopy (TIRFM) demonstrated that CTLs recruited acidic SLs displaying only mCherry fluorescence to the IS with activating SLB. This was rapidly followed (within 1 min) by appearance of SEpHluorin

puncta in the IS (Fig. 1B, Fig. S2, Movie S4). Consistent with release of Gzmb in a SMAP, the SEpHluorin signal persisted in the IS for 20 minutes rather then dispersing.

We next determined if the SMAPs remained attached to the SLB after removal of the CTLs (Fig. 1C, Movie S5). Untransfected CTLs were incubated on the activating SLB, and either directly prepared for immunofluorescence detection of Prf1 and Gzmb or the cells were removed prior to analysis (Fig. 1D). Prf1 and Gzmb immunoreactivity were detected in the IS within 20 minutes, due to the kinetics of antibody binding (Figs. S3-4; Movies S6-9), and remained as discrete particles attached to the SLB after the CTLs were removed (Fig. 1D). The SMAPs were stable without loss of Prf1 and Gzmb for hours without fixation (Fig. S5). We next tested SMAPs for their ability to kill target cells in a cytotoxicity assay based on release of the cytoplasmic enzyme lactate dehydrogenase (LDH). Target cells were killed by SLB immobilized SMAPs (Fig. 1E, black circles) after correction for “spontaneous release” of LDH by target cells (Fig. 1E, red circles). We also confirmed that SMAPs lacked LDH activity (Fig, 1E, blue triangles). Thus, SMAPs are stable after release from CTLs and can kill cells autonomously.

SMAPs captured on SLB were subjected to mass spectrometry (MS) analysis. We identified over 285 proteins that were consistently present in SMAPs (Fig. 2A, B). Of these, 82 were unique to SMAPs on SLB with ICAM-1 and anti-CD3ε versus ICAM-1 alone and 18 proteins were detected in a majority of experiments (Fig. S6). One peptide from Prf1 was detected in multiple experiments and multiple Gzmb peptides were identified in all experiments (Fig. S6). We also identified a number of proteins involved in cell signaling (cytokines and chemokines) (Fig. S6). The presence of Prf1 and Gzmb in SMAPs was further confirmed by SDS-PAGE and immuno-blotting (Fig S7). Plasma membrane proteins such as the phosphatase CD45 and the degranulation marker LAMP-1

(CD107a) were not detected (Fig. S7). This suggested minimal contamination with cellular membranes. LFA-1 was confirmed by immune-blotting, but not by immunofluorescence of SMAPs and thus may represent adhesion sites left on the SLB in parallel with SMAPs (*19*). Thrombospondin-1 (TSP-1) stood out as a candidate based on its signature Ca^{2+} binding repeats (*20, 21*), which resonated with well-established Ca^{2+} dependent steps in CTL mediated killing (*22*). Live imaging of the release of SMAPs on activating SLB showed that TSP-1 and Prf1 are released together (Fig. S8; Movie S10). In addition, TIRFM on SMAPs from CTLs transfected with full length TSP-1 with a C-terminal GFPSpark revealed co-localization of the GFP signal with Gzmb and Prf1 antibody staining in the SMAPs (Fig. 2C; Fig. S9), and anti-TSP-1 antibody staining co-localized with mCherry and pHluorin signals from CTLs transfected with Gzmb-mCherry-pHluorin (Fig. S10). TSP-1-GFPSpark and Gzmb-mCherry-SEpHluorin were co-localized within cytoplasmic compartments in co-transfected CTLs (Fig. S11, Movie S11). This result suggested that SMAPs were preformed and stored in SLs. Enzyme-linked immunosorbent assays on soluble and SLB fractions from stimulation of primary $CD8^+CD57^+$ CTLs revealed similar levels of Gzmb and Prf1 in both fractions, but the dependence on anti-CD3ε stimulation was higher for the SLB fraction (Fig. S12). In contrast, TSP-1 was almost exclusively in the SLB fraction, and displayed significant dependence on anti-CD3ε stimulation (Fig. S12). When we analyzed TSP-1 protein by SDS-PAGE and immuno-blotting we found that CTLs and SMAPs contained not the full-length, 145 kDa species stored in platelets, but a C-terminal 60 kDa fragment under non-reducing and reducing conditions, which included the Ca^{2+} binding repeats (Fig. S13) (*23*). CRISPR/Cas9 mediated knockout of TSP-1 by 60% in CTLs reduced anti-CD3ε redirected killing of K562 cells by 30% ($n = 5$, $p < 0.001$), whereas knockout of another similarly enriched protein, galectin-1, by 90% had no effect on killing (Fig. 2D, E). While TSP-1 is associated with T cell adhesion to

extracellular matrix (*24*), TSP-1 knockout did not alter T cell adhesion to activating SLB, but did reduce the signals for TSP-1, Prf1 and Gzmb in SMAPs (Fig S14). These results suggested that the C-terminal domain of TSP-1 was a component of SMAPs and is important in CTL mediated killing.

We next investigated the organization of molecules within SMAPs at 20 nm resolution by direct Stochastic Optical Reconstruction Microscopy (dSTORM). SMAPs were detected with WGA in clusters of 27 ± 12 SMAPs per IS (Fig. 3A). On closer inspection, WGA staining appeared as a dense ring in the 2D projections, which indicated a spherical shell with an average diameter of 120 ± 43 nm (Fig. 3A). Many supramolecular assemblies use phospholipid bilayers as a scaffold and thus we asked if SMAPs stain with the lipophilic membrane dye DiD, which brightly stains extracellular vesicles or lipoproteins. DiD did not stain SMAPs, consistent with the paucity of membrane proteins detected in the mass spectrometry (Fig. S15). Thus, the WGA staining pattern was most consistent with a shell of glycoproteins (*16*), rather than a phospholipid-based membrane surrounding SMAPs. The location of TSP-1 in SMAPs was investigated by multicolor dSTORM. Strikingly, TSP-1 co-localized with WGA (59 ± 3 %) and similarly highlighted the shape of the SMAPs (Fig. 3B; Fig. S16). Thus, SMAPs from CTLs have a glycoprotein shell that includes TSP-1.

To further investigate the structure of SMAPs, we used Cryo-Soft X-ray Tomography (CSXT), a non-destructive 3D method based on the preferential absorption of X-rays by carbon rich cellular structures within unstained, vitrified specimens with a resolution of 40 nm (*25*, *26*). For this, CTLs were incubated on EM grids coated with ICAM-1 and anti-CD3ε. After incubation, samples were

plunge-frozen with the T-cells in place or removed to leave only the SMAPs. Released SMAPs captured on the grid after cell removal (Fig. 3C; Movie S12) were readily resolved and had an average diameter of 111 ± 36 nm (Fig. S17). The slightly larger size of SMAPs by dSTORM reflects the contribution of ~9 nm based on the 2.45 nm hydrodynamic radius of WGA. The carbon dense shell observed in CSXT was consistent with the TSP-1/WGA shell observed by dSTORM. The CSXT analysis further emphasized intracellular multicore granules in the CTLs that appeared to be tightly packed with SMAPs, where the lower density cores were resolved (Movie S13). These multicore granules were associated with the basal surface of CTLs near activating grids (Fig. 3D; Movie S14), as expected (*3*).

We next undertook 3-color dSTORM to determine the location of cytotoxic proteins within SMAPs. The TSP-1/WGA shell enclosed partly overlapping Prf1 and Gzmb positive areas across the 2D projection (Fig. 4A,B). We also detected Srgn in the core of SMAPs (Fig S18). Given the apparent density of material in the shell and stability of SMAPs, it was surprising that 150 kDa antibodies had access to components in the core. This is an unexpected property that will require further investigation. SMAPs containing Prf1 and/or Gzmb were bigger and more abundant than WGA^+ particles devoid of cytotoxic proteins (Fig. 4C, D). Primary $CD8^+CD57^+$ CTLs and NK cells from peripheral blood also released SMAPs with Prf1, Gzmb and TSP-1 (Fig S19). These results completed our picture of SMAPs as being autonomously cytotoxic, ~120 nm in diameter with a dense shell including TSP-1, a core of Prf1, Gzmb and Srgn and surprising accessibility to antibodies.

CTLs can also use the ligand for the death receptor Fas (FasL) to kill targets expressing Fas (*27*). We only detected FasL in the CTL IS when Fas glycoprotein was incorporated in the SLB with ICAM-1 and anti-CD3ε (Fig S20). In these cases, FasL distribution in the IS was in puncta distinct from Prf1 and Gzmb. The related protein CD40L is released in a CD40 dependent manner in helper T-cell IS within synaptic ectosomes (*28, 29*). Synaptic ectosomes are a type of extracellular vesicle similar to exosomes, but generated by budding from the plasma membrane of the T-cell in the IS (*29, 30*). These results suggested that there were two types of cytotoxic particles released by CTLs in contact with Fas expressing targets – FasL clusters in vesicles and SMAPs.

Our working model for SMAP function is that they act as autonomous killing entities with innate targeting through TSP-1 and potentially other shell components. While SMAPs transferred through the IS may only impact one target, CTLs can kill without an IS using a process involving rapid contacts (*14, 31*). The ability of SMAPs to autonomously kill target cells may become important in situations of transient and multiple interactions where delivery might be less precise. SMAPs may have other modes of action potentially including chemoattraction through CCL5 and immune modulation through IFNγ. The TSP-1 C-terminus contains the binding site for the ubiquitous “don’t eat me” signal CD47 (*32*). SMAPs may thus partner with myeloid cells to ensure that any cell that cannot be killed by SMAPs is culled by phagocytosis (*33*).

References and Notes:

1. D. Masson, J. Tschopp, A family of serine esterases in lytic granules of cytolytic T lymphocytes. *Cell* **49**, 679-685 (1987).

2. J. Tschopp, S. Schafer, D. Masson, M. C. Peitsch, C. Heusser, Phosphorylcholine acts as a Ca2+-dependent receptor molecule for lymphocyte perforin. *Nature* **337**, 272-274 (1989).

3. J. C. Stinchcombe, G. Bossi, S. Booth, G. M. Griffiths, The immunological synapse of CTL contains a secretory domain and membrane bridges. *Immunity* **15**, 751-761. (2001).

4. G. Menasche, J. Feldmann, A. Fischer, G. de Saint Basile, Primary hemophagocytic syndromes point to a direct link between lymphocyte cytotoxicity and homeostasis. *Immunol Rev* **203**, 165-179 (2005).

5. M. Kalos *et al.*, T cells with chimeric antigen receptors have potent antitumor effects and can establish memory in patients with advanced leukemia. *Sci Transl Med* **3**, 95ra73 (2011).

6. C. J. Froelich *et al.*, New paradigm for lymphocyte granule-mediated cytotoxicity. Target cells bind and internalize granzyme B, but an endosomolytic agent is necessary for cytosolic delivery and subsequent apoptosis. *J Biol Chem* **271**, 29073-29079 (1996).

7. D. Keefe *et al.*, Perforin triggers a plasma membrane-repair response that facilitates CTL induction of apoptosis. *Immunity* **23**, 249-262 (2005).

8. R. H. Law *et al.*, The structural basis for membrane binding and pore formation by lymphocyte perforin. *Nature* **468**, 447-451 (2010).

9. S. S. Metkar *et al.*, Cytotoxic cell granule-mediated apoptosis: perforin delivers granzyme B-serglycin complexes into target cells without plasma membrane pore formation. *Immunity* **16**, 417-428 (2002).

10. J. A. Martina *et al.*, Imaging of lytic granule exocytosis in CD8+ cytotoxic T lymphocytes reveals a modified form of full fusion. *Cell Immunol* **271**, 267-279 (2011).

11. P. J. Peters *et al.*, Molecules relevant for T cell-target cell interaction are present in cytolytic granules of human T lymphocytes. *Eur J Immunol* **19**, 1469-1475 (1989).

12. P. J. Peters *et al.*, Cytotoxic T lymphocyte granules are secretory lysosomes, containing both perforin and granzymes. *J Exp Med* **173**, 1099-1109 (1991).

13. L. Lugini *et al.*, Immune surveillance properties of human NK cell-derived exosomes. *J Immunol* **189**, 2833-2842 (2012).

14. F. Bertrand *et al.*, An initial and rapid step of lytic granule secretion precedes microtubule organizing center polarization at the cytotoxic T lymphocyte/target cell synapse. *Proc Natl Acad Sci U S A* **110**, 6073-6078 (2013).

15. W. T. Kim *et al.*, Delayed reentry of recycling vesicles into the fusion-competent synaptic vesicle pool in synaptojanin 1 knockout mice. *Proc Natl Acad Sci U S A* **99**, 17143-17148 (2002).

16. R. Kornfeld, S. Kornfeld, Assembly of asparagine-linked oligosaccharides. *Annu Rev Biochem* **54**, 631-664 (1985).

17. G. M. Griffiths, S. Isaaz, Granzymes A and B are targeted to the lytic granules of lymphocytes by the mannose-6-phosphate receptor. *J Cell Biol* **120**, 885-896 (1993).

18. K. Somersalo *et al.*, Cytotoxic T lymphocytes form an antigen-independent ring junction. *J Clin Invest* **113**, 49-57 (2004).

19. J. C. Kuo, X. Han, C. T. Hsiao, J. R. Yates, 3rd, C. M. Waterman, Analysis of the myosin-II-responsive focal adhesion proteome reveals a role for beta-Pix in negative regulation of focal adhesion maturation. *Nat Cell Biol* **13**, 383-393 (2011).

20. M. Kvansakul, J. C. Adams, E. Hohenester, Structure of a thrombospondin C-terminal fragment reveals a novel calcium core in the type 3 repeats. *EMBO J* **23**, 1223-1233 (2004).

21. T. M. Misenheimer, D. F. Mosher, Calcium ion binding to thrombospondin 1. *J Biol Chem* **270**, 1729-1733 (1995).

22. E. R. Podack, P. J. Konigsberg, Cytolytic T cell granules. Isolation, structural, biochemical, and functional characterization. *J Exp Med* **160**, 695-710 (1984).

23. D. S. Annis, J. E. Murphy-Ullrich, D. F. Mosher, Function-blocking antithrombospondin-1 monoclonal antibodies. *J Thromb Haemost* **4**, 459-468 (2006).

24. S. S. Li *et al.*, T lymphocyte expression of thrombospondin-1 and adhesion to extracellular matrix components. *Eur J Immunol* **32**, 1069-1079 (2002).

25. G. Schneider, Cryo X-ray microscopy with high spatial resolution in amplitude and phase contrast. *Ultramicroscopy* **75**, 85-104 (1998).

26. M. Harkiolaki *et al.*, Cryo-soft X-ray tomography: using soft X-rays to explore the ultrastructure of whole cells. *Emerging Topics in Life Sciences*, ETLS20170086 (2018).

27. G. Bossi, G. M. Griffiths, Degranulation plays an essential part in regulating cell surface expression of Fas ligand in T cells and natural killer cells. *Nat Med* **5**, 90-96 (1999).

28. K. Choudhuri *et al.*, Polarized release of T-cell-receptor-enriched microvesicles at the immunological synapse. *Nature* **507**, 118-123 (2014).

29. D. G. Saliba *et al.*, Composition and structure of synaptic ectosomes exporting antigen receptor linked to functional CD40 ligand from helper T-cells. *eLife* **8**, 600551 (2019).

30. E. Cocucci, J. Meldolesi, Ectosomes and exosomes: shedding the confusion between extracellular vesicles. *Trends Cell Biol* **25**, 364-372 (2015).

31. S. Halle *et al.*, In Vivo Killing Capacity of Cytotoxic T Cells Is Limited and Involves Dynamic Interactions and T Cell Cooperativity. *Immunity* **44**, 233-245 (2016).

32. V. Mateo *et al.*, CD47 ligation induces caspase-independent cell death in chronic lymphocytic leukemia. *Nat Med* **5**, 1277-1284 (1999).

33. P. A. Oldenborg, H. D. Gresham, F. P. Lindberg, CD47-signal regulatory protein alpha (SIRPalpha) regulates Fcgamma and complement receptor-mediated phagocytosis. *J Exp Med* **193**, 855-862 (2001).

34. M. L. Dustin, T. Starr, R. Varma, V. K. Thomas, Supported planar bilayers for study of the immunological synapse. *Curr Protoc Immunol* **Chapter 18**, Unit 18.13 (2007).

35. M. Bates, G. T. Dempsey, K. H. Chen, X. Zhuang, Multicolor super-resolution fluorescence imaging via multi-parameter fluorophore detection. *Chemphyschem* **13**, 99-107 (2012).

36. S. Balint, I. Verdeny Vilanova, A. Sandoval Alvarez, M. Lakadamyali, Correlative live-cell and superresolution microscopy reveals cargo transport dynamics at microtubule intersections. *Proc Natl Acad Sci U S A* **110**, 3375-3380 (2013).

37. F. B. Lopes *et al.*, Membrane nanoclusters of FcgammaRI segregate from inhibitory SIRPalpha upon activation of human macrophages. *J Cell Biol* **216**, 1123-1141 (2017).

38. M. Bates, B. Huang, G. T. Dempsey, X. Zhuang, Multicolor super-resolution imaging with photo-switchable fluorescent probes. *Science* **317**, 1749-1753 (2007).

39. B. Huang, W. Wang, M. Bates, X. Zhuang, Three-dimensional super-resolution imaging by stochastic optical reconstruction microscopy. *Science* **319**, 810-813 (2008).

40. S. Malkusch *et al.*, Coordinate-based colocalization analysis of single-molecule localization microscopy data. *Histochem Cell Biol* **137**, 1-10 (2012).

41. J. R. Kremer, D. N. Mastronarde, J. R. McIntosh, Computer visualization of three-dimensional image data using IMOD. *J Struct Biol* **116**, 71-76 (1996).

42. A. Cardona *et al.*, TrakEM2 software for neural circuit reconstruction. *PLoS One* **7**, e38011 (2012).

Acknowledgments: We thank E. Kurz, S. Valvo, L. Chen, H. Rada, M. C. Spink, M.P. Puissegur, M. Mixon, J. Love and A. Sessions for important contributions to this work; Prof. B. Alarcon, Prof. C. Baldari, Prof J. Rettig, Dr. E. Abu Shah and Dr. F. Bravo Lopes for advice.

Funding: Supported by the ERC AdG 670930 (MLD), the Wellcome Trust 100262 (MLD) and the Kennedy Trust (to MLD and BMK); the Laboratoire d'Excellence Toulouse Cancer (TOUCAN) under contract ANR11-LABX and Ligue Nationale contre le Cancer (Equipe labellisée 2018) (to SV); the Institute for Protein Innovation, and STFC and Wellcome for support of Diamond Light Source Ltd.

Author contributions: SB and MLD conceived study and designed experiments. SB performed experiments and analyzed data. SM and SV performed CTL clone experiments. RF and BMK acquired and analyzed Mass Spectroscopy data. MH acquired and analyzed CSXT data. SB and MLD wrote the manuscript.

Competing interests: M. Dustin and S. Balint have filed a provisional patent on SMAP isolation and engineering.

Data and materials availability: All data are available in the manuscript or the supplementary material.

Supplementary Materials:

Materials and Methods

Figures S1-S20

Movies S1-S14

Data S1

References *(34-42)*

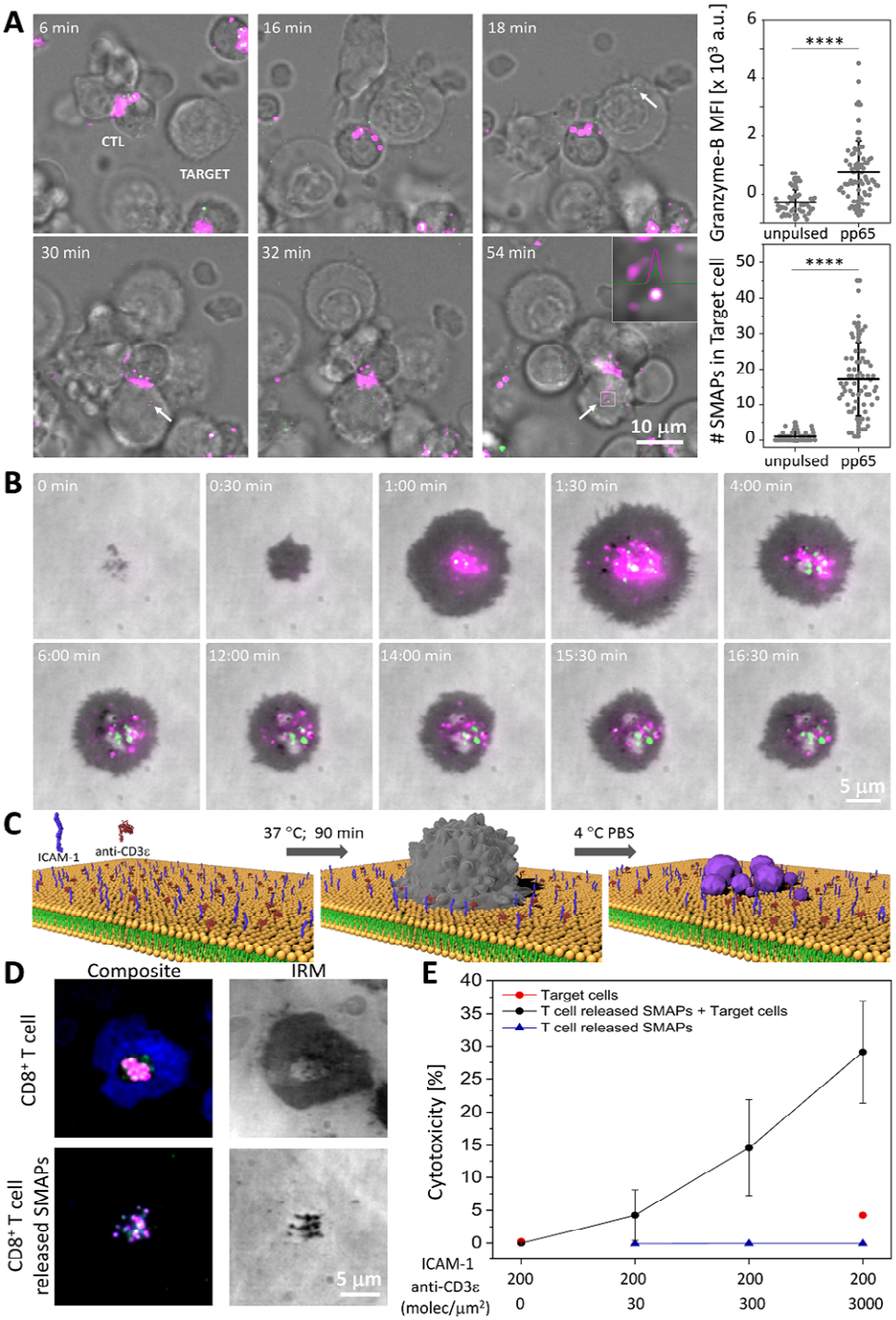

Fig. 1. SMAPs were released at the IS and displayed autonomous cytotoxicity. (A) Time-lapse confocal images depicting the transfer of Gzmb-mCherry^{+} (green) and WGA (magenta) labeled SMAPs from an antigen-specific CTL clone into pp65-pulsed JY target cells (Target). Arrows and

inset indicate the presence of SMAPs inside the target. Scale bar, 10 μm. Quantification of Gzmb mean fluorescence intensity (MFI) and number of double-positive particles inside the target cell in CTL conjugates with unpulsed or pulsed target cells. Each dot represents one target cell (< 50 cells). Horizontal lines and error bars represent mean ± SD from 2 independent experiments. ****, $p < 0.0001$ (B) Live cell imaging of SMAPs release by $CD8^+$ T-cells transfected with Gzmb-mCherry-SEpHluorin (magenta/green) on activating SLB. IRM, interference reflection microscopy. Scale bar, 5 μm. (C) Schematic of the working model for capturing SMAPs released by activated $CD8^+$ T-cells. $CD8^+$ T-cells (grey) were incubated on SLB presenting activating ligands for the indicated time. Cells were removed with cold PBS leaving the released SMAPs (purple) on the SLB. Elements are not drawn to scale. (D) TIRFM images of $CD8^+$ T-cells incubated on activating SLB in the presence of anti-Prf1 (green) and anti-Gzmb (magenta) antibodies (top panels). After cell removal, $Prf1^+$ and $Gzmb^+$ SMAPs remained on the SLB (bottom panels). The formation of a mature IS is indicated by an ICAM-1 ring (blue). IRM, interference reflection microscopy. Scale bar, 5 μm. (E) Target cell cytotoxicity induced by density-dependent release of SMAPs captured on SLB measured by LDH release assay. Data points and error bars represent mean ± SEM from 3 independent experiments.

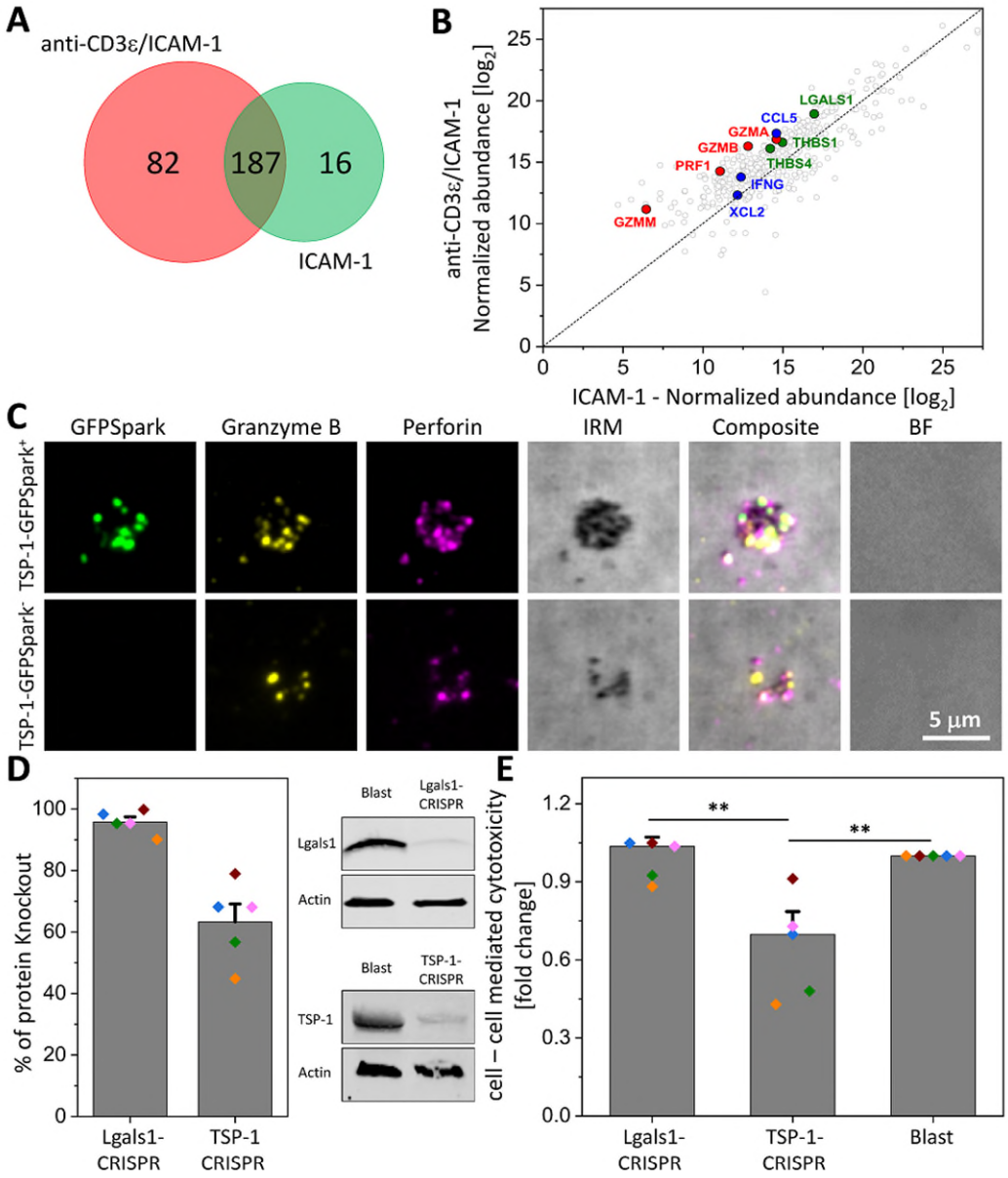

Fig. 2. TSP-1 was a major constituent of SMAPs and contributed to CTL killing of targets. (A) Two-set Venn diagram showing the number of individual and common proteins identified by MS analysis of material released by $CD8^+$ T-cells incubated on non-activating (ICAM-1) or activating (ICAM-1 + anti-CD3ε) SLB. Representative of 3 independent experiments with 8 donors. (B) Normalized abundance of the 285 proteins identified by MS in each condition.

Cytotoxic proteins are highlighted in red, chemokine/cytokines in blue and adhesion proteins in green. (C) TIRFM images of SMAPs released from $CD8^+$ T-cells transfected with TSP-1-GFPSpark (green; top row) or non-transfected cells (bottom row). Released SMAPs were further stained with anti-Gzmb (yellow) and anti-Prf1 (magenta) antibodies. IRM, interference reflection microscopy. BF, bright field microscopy. Scale bar, 5 μm. (D) Percentage of galectin-1 and TSP-1 knockout in $CD8^+$ T-cells by CRISPR/Cas9 genome editing measured from immuno-blotting analysis (left). Each colored dot represents one donor. Bars represent mean ± SEM. Representative immuno-blot for galectin-1 (Lgals1) and TSP-1 in Lgals1 and TSP-1, respectively edited $CD8^+$ T-cells (right). $CD8^+$ T-cells (Blast) were analyzed in parallel as a control. (E) Target cell cytotoxicity mediated by galectin-1 (Lgals1-CRISPR) or TSP-1 (TSP-1-CRISPR) gene edited $CD8^+$ T-cells measured by LDH release assay. T cell blasts were used as a control. Bars represent mean ± SEM. **, $p < 0.01$. Donors are the same as in (D).

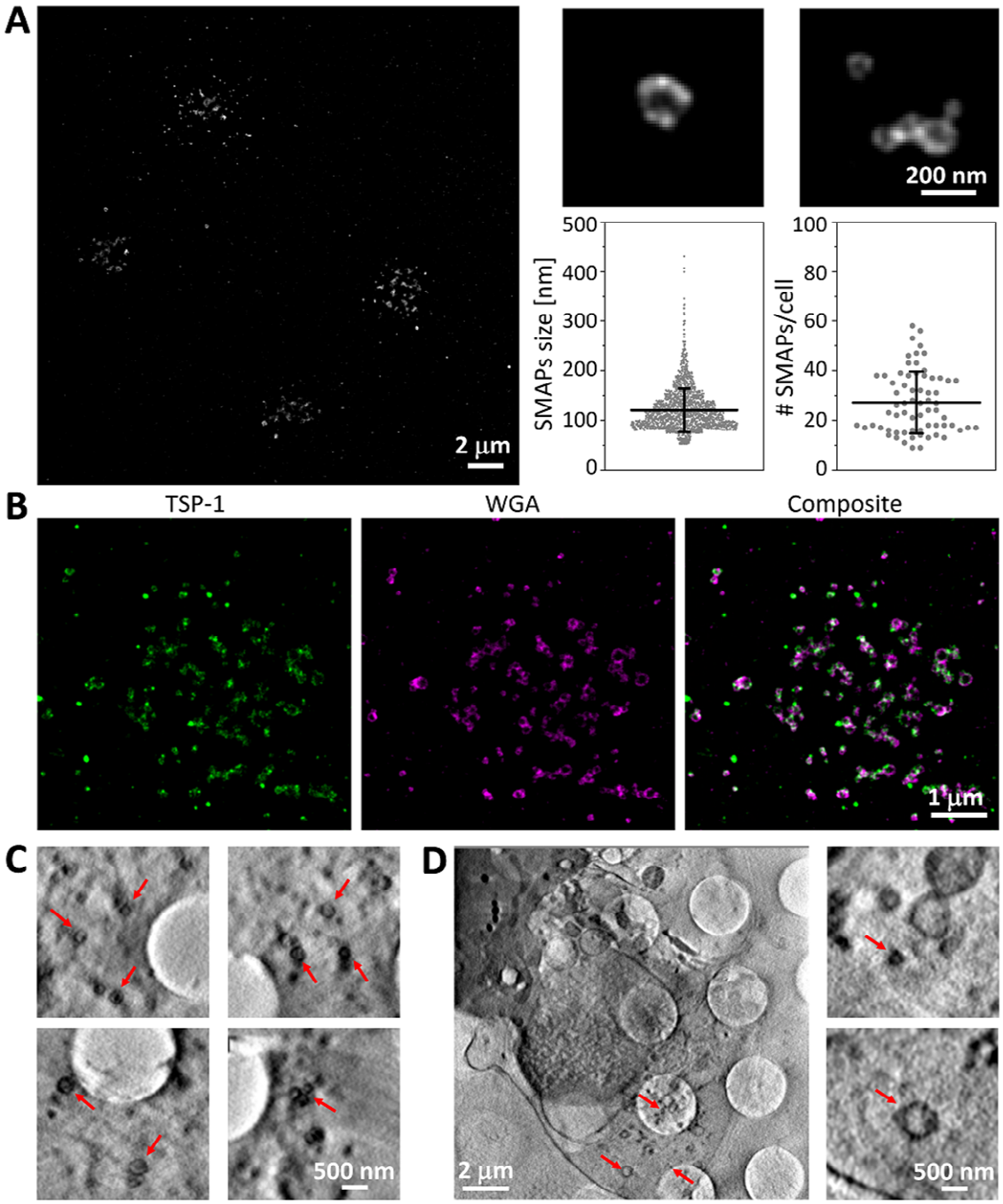

Fig. 3. SMAPs shell was rich in glycoproteins, TSP-1 and organic material. (A) dSTORM image of SMAPs released on activating SLB by multiple cells (left; scale bar, 2 µm) and two examples of individual SMAPs (top right; scale bar, 200 nm), showing their heterogeneity in size. SMAPs were labeled with WGA. Quantification of SMAPs size and number released per cell

(bottom right; n>1800 and n=67, respectively). Horizontal lines and error bars represent mean ± SD from five donors. (B) dSTORM images of SMAPs (labeled with WGA, magenta) positive for TSP-1 (green) released on activating SLB. Scale bar, 1 μm. (C) Multiple CSXT examples of released SMAPs after cell removal. Scale bar, 500 nm. (D) CSXT of $CD8^+$ T-cells interacting with carbon coated EM grids (note grid holes in C and D) containing ICAM-1 and anti-CD3ε. Scale bar, 2 μm or 500 nm for zoomed in regions (right). Arrows indicate SMAPs.

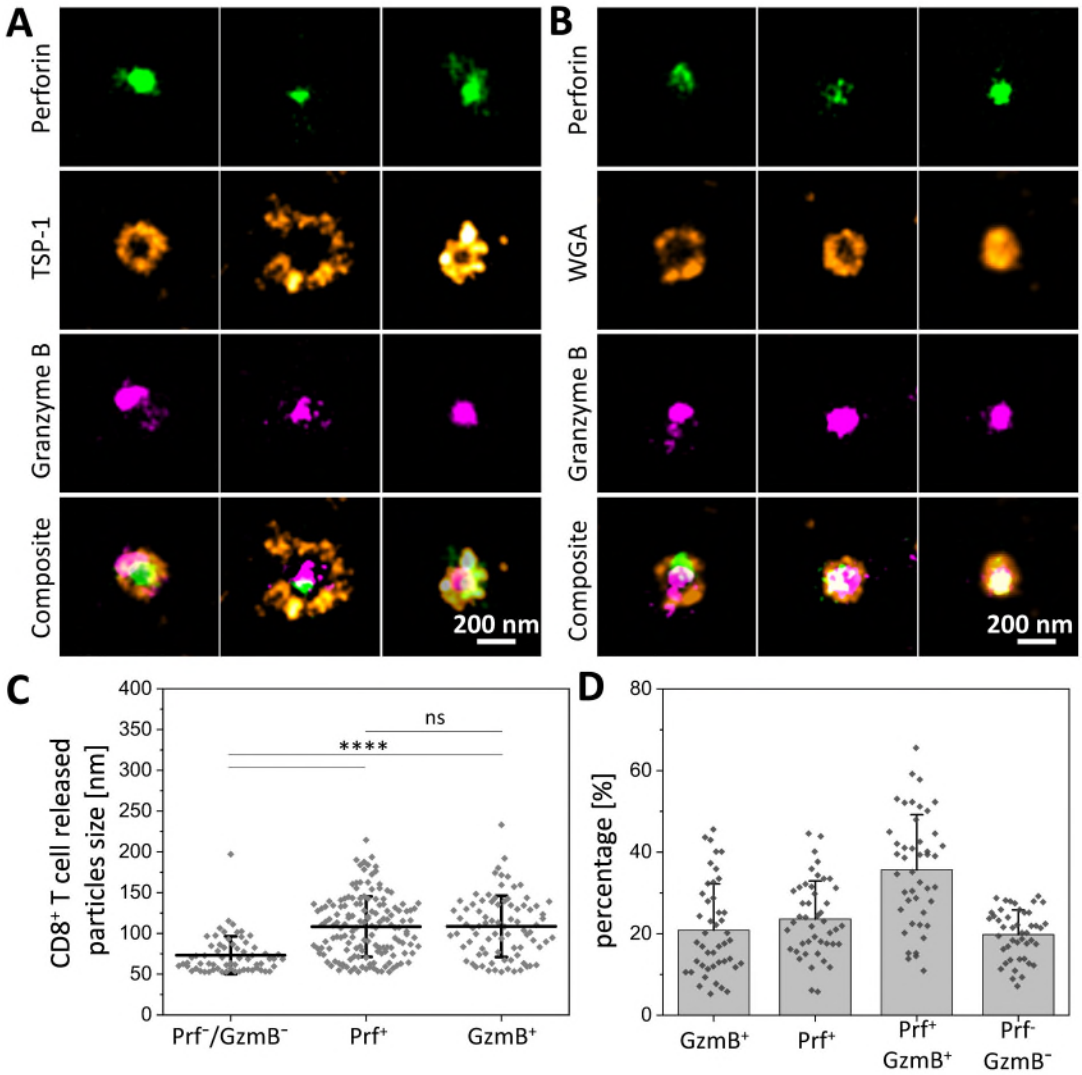

Fig. 4. SMAPs had a TSP-1 shell and a core of cytotoxic proteins. (A and B) dSTORM images of individual SMAPs positive for Prf1 (green), Gzmb (magenta) and TSP-1 (A, orange) or stained with WGA (B, orange). Scale bar, 200 nm. (C) Quantification of the size of cytotoxic particles based on their protein composition (n=64 for $Prf1^-$ and $Gzmb^-$ cytotoxic particles, n=149 and n=83 for $Prf1^+$ and $Gzmb^+$ cytotoxic particles, respectively). ****, $p < 0.0001$. n.s, not significant. (D)

Quantification of the percentage of particles positive and negative for Prf1 or Gzmb. (C-D) Horizontal lines/bars and error bars represent mean ± SD from five donors.

Science
AAAS

Supplementary Materials for

Supramolecular attack particles are autonomous killing entities released from cytotoxic T-cells

Š. Balint, S. Müller, R. Fischer, B. M. Kessler, M. Harkiolaki, S. Valitutti and M. L. Dustin*

Correspondence to: michael.dustin@kennedy.ox.ac.uk

This PDF file includes:

Materials and Methods

Generation of Cytotoxic T-cells (CTLs)

Peripheral blood from healthy donors was acquired from the National Health Service blood service under ethics license REC 11/H0711/7 (University of Oxford). $CD8^+$ T-cells were isolated by negative selection (RosetteSep^{TM} Human $CD8^+$ T-cell Enrichment Cocktail, STEMCELL technologies, Cambridge, UK; #15023) following the manufacturer's protocol. $CD8^+$ T-cells were activated by using anti-CD3/anti-CD28 T-cell activation and expansion beads (Dynabeads ThermoFisher Scientific, Loughborough, UK; #11132D) in complete R10 medium (RPMI 1640 (#31870074), 10% FBS (#A3160801), 1% Penicillin-Streptomycin (#15140122), 1% L-Glutamine (#25030024), 25 mM HEPES (#15630080), 1% Non-essential amino acids (#11140035) all from ThermoFisher Scientific) supplemented with 50 Units/mL of recombinant human IL-2 (PeproTech, London, UK; #200-02). After three days of incubation the beads were removed, and the cells were seeded with 35 Units/mL of IL-2 in complete R10 medium at 10^6 cells/mL for further two days. The activated and rested $CD8^+$ T-cells are referred to as "$CD8^+$ T-cells" and were used within the following two days as a source enriched in CTL.

Isolation of primary NK cells and primary CTLs

Primary NK cells were isolated by negative selection (RosetteSep^{TM} Human NK cell Enrichment Cocktail, STEMCELL technologies; #15065) following the manufacturer's protocol. Primary CTLs, defined as $CD8^+$ $CD57^+$ T-cells, were isolated from total $CD8^+$ T-cells, as described above, by positive selection with $CD57^+$ magnetic beads (Miltenyi Biotec, Woking, UK; #130-092-073) following the manufacturer's protocol. Cells were kept in complete R10 medium without IL-2 and used immediately.

Generation of CTL clones

Human $CD8^+$ T-cells were purified from healthy donor blood samples using the RosetteSep Human $CD8^+$ T Cell Enrichment Cocktail. For cloning, HLA-A2-restricted $CD8^+$ T-cells specific for the NLVPMVATV peptide of the cytomegalovirus protein pp65 were tetramer stained and single cell sorted into 96-U-bottom plates using a BD FACSAria II cell sorter. Cells were cultured in RPMI/HS (RPMI 1640 medium supplemented with 5% human AB serum (Institut de Biotechnologies Jacques Boy, Reims, FR), minimum essential amino acids, HEPES and sodium pyruvate, 150 Units/mL human recombinant IL-2 and 50 ng/mL human recombinant IL-15). $CD8^+$ T-cell clones were stimulated in complete RPMI/HS medium containing 1 µg/mL PHA with 1 x 10^6/mL 35 Gy irradiated allogeneic peripheral blood mononuclear cells which were isolated by Ficoll-Paque centrifugation from fresh heparinized blood samples of healthy donors obtained from Etablissement Francais du Sang and 1 x 10^5/mL 70 Gy irradiated EBV-transformed B cells. Re-stimulation of clones was performed every 2 weeks. Blood samples were collected and processed following standard ethical procedures (Helsinki protocol), after obtaining written informed consent from each donor and approval by the French Ministry of the Research (transfer agreement AC-2014-2384). Approbation by the ethical department of the French Ministry of the Research for the preparation and conservation of cell lines and clones starting from healthy donor human blood samples has been obtained (authorization No DC-2018-3223).

EBV-transformed B cells (JY) HLA-$A2^+$ were used as target cells and cultured in RPMI 1640 GlutaMAX supplemented with 10% FCS and 50 µM 2-mercaptoethanol, 10 mM HEPES, 1X MEM non-essential amino acids, 1X sodium pyruvate, 10 µg/mL ciprofloxacine. All cell lines are routinely screened for mycoplasma contamination using MycoAlert mycoplasma detection kit (Lonza, Basel, SW).

Protein purification

UCHT1 anti-CD3ε Fab were prepared from UCHT1 IgG (Bio X cell, Lebanon, NH) by pepsin digestion followed by gel filtration, reduction of the hinge disulfides and reaction with maleimide-PEG2-biotin (Thermo Fisher Scientific; #21901BID). These were then labeled with NHS esters of fluorescent dyes at ~1 fluorophore per Fab ratio. Recombinant ICAM-1-12His was generated in S9 cells, purified by Ni^{2+} affinity and labeled with AlexaFluor405-NHS ester. Recombinant Fas-10His was expressed in Freestyle 293 expression system (Thermo Fisher Scientific), purified by Ni^{2+} affinity and labeled with AlexaFluor647-NHS ester (Thermo Fisher Scientific).

Supported lipid bilayer (SLB)

Preparation of liposomes and mobile SLB formation were described in detail elsewhere (*34*). Small unilamellar vesicles (average 80 nm by nanoparticle tracking analysis) with 12.5 mol% DOGS-NTA and 0.02 mol% of DOPE-CAP-Biotin (to yield 30 molecules/μm^2 anti-CD3ε-Fab) in DOPC at a total lipid concentration of 0.4 mM were prepared by extrusion. All lipids and the extrusion systems were obtained from Avanti Polar Lipids (Alabaster, AL). SLB were deposited onto clean glass coverslip (SCHOTT UK Ldt, Stafford, UK; #1472315) affixed with a flow chamber (sticky-Slide VI 0.4, Ibidi, Thistle Scientific LTD, Glasgow, UK; #80608) by filling the channels with liposome suspension. After 20 min incubation the channels were injected with 5 mL each of HEPES Buffered Saline (HBS) supplemented with 0.1% Human Serum Albumin (HSA) (Merck-Millipore, Watford, UK; #12667-50mL) to remove excess liposomes without introducing air bubbles. After blocking with 5% casein in PBS containing 100 μM $NiSO_4$, 10 μg/mL unlabeled streptavidin (Europa Bioproducts Ltd, Ipswich, UK; #PZSA10-100) was coupled to biotin head groups for 15 min. SLB were flushed with HSA/HBS and incubated for 20 min with 200

molecules/μm^2 of ICAM-1-AlexaFluor405-His tagged protein (non-activating condition) or with an addition of 5 μg/mL of anti-CD3ε-Fab (activating condition). Unbound proteins were flushed out by HSA/HBS and the SLB were ready to use. SLB were uniformly fluid as determined by fluorescence recovery after photobleaching. Protein concentrations required to achieve desired densities on bilayers were calculated from calibration curves constructed from flow cytometric measurements of bilayer-associated fluorescence of attached proteins on bilayers formed on glass beads, compared with reference beads containing known numbers of the appropriate fluorophore (Bangs Laboratories, Fishers, IN; #647-A).

Release of Supramolecular Attack Particles (SMAPs)

$CD8^+$ T-cells, primary NK cells and primary CTLs were plated onto activating or non-activating SLB for 90 min at 37°C. After incubation, cells were flushed out for a minimum of three times with ice-cold PBS. The released SMAPs were thus captured on SLB and were further analyzed by ELISA, immunostaining or immuno-blotting.

Transfection of $CD8^+$ T-cells

$CD8^+$ T-cells were activated with anti-CD3/anti-CD28 T-cell activation and expansion beads in complete R10 medium supplemented with 50 Units/mL of IL-2. After two or three days of incubation the beads were removed and the cells were transfected with mRNA or cDNA, and cultured with 35 Units/mL of IL-2 in complete R10 medium at 10^6 cells/mL. 0.2 x 10^6 $CD8^+$ T-cells were transfected with 2 μg Gzmb-mCherry-SEpHluorin mRNA and/or 2 μg TSP-1-GFPSpark cDNA (Sino Biological; Stratech Scientific Ltd., Cambridge, UK #HG10508-ACG) by

using the Neon Transfection system (ThermoFisher Scientific), electrical pulse 1600V, 10 ms and 3 pulses in 10 μL buffer R. The transfection efficiency was assessed after 24 hours.

Transfection of CTL clones

For efficient transfection of human CTLs with tagged molecules, we synthetized capped and poly(A) tailed mRNA by in vitro transcription from the plasmid pGzmb-mCherry-SEpHluorin. 1 μg of pGzmb-mCherry-SEpHluorin was first linearized by NotI digestion to be used as template for in vitro transcription by the T7 RNA polymerase using mMESSAGE mMACHINE T7 Ultra kit (Thermo Fisher) as per manufacturer's protocol.

Human CTL clones were transfected using a GenePulser Xcell electroporation system (BioRad, Kidlington, UK). $1x10^6$ CTLs (5 days after restimulation and therefore in expansion phase) were washed and resuspended in 100 μL Opti-MEM medium at room temperature with 2 μg mRNA (*square wave* electrical pulse at 300V, 2ms, 1 pulse). 16 hours after transfection the transfection efficiency was verified by FACS analysis (typically 50-80% of cells were transfected).

Total Internal Reflection Fluorescent Microscopy (TIRFM) imaging

TIRFM imaging was performed with an Olympus IX83 inverted microscope (Keymed, Southend-on-Sea, UK) equipped with a 150× 1.45 NA oil-immersion objective. For TIRFM imaging, cells were plated onto activating or non-activating SLB for 5, 10, 20 or 30 min and then fixed with 4% PFA/PBS for 30 min at room temperature. After fixation the cells were stained for one hour with 10 μg/mL directly conjugated anti-Gzmb-AlexaFluor647 (BD Biosciences; #560212), in-house labeled anti-TSP-1-AlexaFluor647 (Abcam, Cambridge, UK; #1823) and anti-Prf1-AlexaFluor488 (BD Biosciences, Wokingham, UK; #563764) primary antibodies after blocking

with 5% BSA/PBS for one hour. Wheat Germ Agglutinin (WGA) conjugated with CF568 (Biotium, Fremont, CA; #29077-1) or AlexaFluor488 (ThermoFisher Scientific, Waltham, MA; #W11261), or DiD/DiI (ThermoFisher Scientific; #V22887/#V22888) membrane dyes were used to label the cell membrane or the $CD8^+$ T-cell released SMAPs. Fluorescent emission was collected by the same objective onto an electron-multiplying charge-coupled device camera (Evolve Delta, Photometrics, Tuscon, AZ). Post processing of the fluorescence images was performed with ImageJ (National Institute of Health).

Live cell TIRFM imaging

Live cell TIRFM imaging was performed with an Olympus IX83 inverted microscope (Keymed, Southend-on-Sea, UK) equipped with a 150× 1.45 NA oil-immersion objective at 37°C. $CD8^+$ T-cells were pre-incubated with anti-Prf1-AlexaFluor488 and anti-Gzmb-AlexaFluor647 or with in house labeled anti-TSP-1-AlexaFluor647 for 20 min on activating SLB before live cell imaging. Cells were recorded every minute for approximately 50 minutes before being flushed out on the stage with ice-cold PBS. A focus lock system was used to keep the sample in focal plane.

For live cell imaging of the fluorescently tagged Gzmb-mCherry-SEpHluorin, the transfected CTLs were plated on activating SLB 24 hours after transfection. The fluorescent emission was recorded every 30 seconds for approximately 20 minutes. Post processing of the fluorescence images and video creation was performed with ImageJ (National Institute of Health).

Live cell confocal imaging

Transfected CTLs were loaded with 1μg/mL AlexaFluor647 conjugated WGA for 4h and extensively washed with 5% FCS/RPMI/10mM HEPES. JY cells were left unpulsed or pulsed

with 10 µM NLVPMVATV peptide, loaded with CTV (Invitrogen, Thermo-Fisher, Loughborough, UK), washed and seeded at 2 x 10^4 cells per well on poly-D-lysine-coated 15-well chambered slides (Ibidi) before imaging. Chambered slides were mounted on a heated stage within a temperature-controlled chamber maintained at 37°C and 5% CO_2 and inspected by time-lapse laser scanning confocal microscopy (LSM 780 or LSM880, Zeiss, Germany).

Confocal imaging

CTL clones and CTV labeled and peptide pulsed or unpulsed JY cells were prepared as for time-lapse live cell confocal microscopy. Transfected CTL clones were conjugated with target cells (1 min, 1500 rpm centrifugation) and incubated for 2h at 37°C, 5% CO_2, in 5% FCS/RPMI/10mM HEPES. Cells were resuspended and seeded on poly-L-lysine coated slides, fixed with 3% PFA/PBS for 15 min at room temperature. Cells were mounted in 90% glycerol/PBS containing 2.5% DABCO (Sigma Aldrich, Dorset, UK) and inspected by using laser scanning confocal microscope (LSM780 or LSM880, Zeiss) with a 63x oil-immersion objective. Post processing of the fluorescence images and *z*-stack creation was performed with ImageJ (National Institute of Health). The number of SMAPs within a target cell was counted manually from 3D z stack reconstructions from 2 independent experiments. Only SMAPs undoubtedly present inside the target cells were counted. Mean fluorescent intensity of the Gzmb-mCherry signal was quantified from the maximum intensity projection of the confocal *z*-stacks highlighting the target cell area.

3D Confocal imaging of the Fas-Fas Ligand was performed by using a Nikon A1R HD25 confocal system with a 60x oil-immersion objective (Nikon, Surbiton, UK). Cells were plated onto activating or non-activating SLB in the presence or absence of in house labeled Fas-AlexaFluor647 and/or unlabeled human CD58 at the concentration of ~200 and/or ~100 molecules/μm^2,

respectively. After 20 min incubation at 37 °C and 5% CO_2 the cells were fixed with 4% PFA/PBS for 30 min at room temperature. After fixation the cells were stained for one hour with 10 µg/mL directly conjugated in house labeled anti−FasLigand-AlexaFluor568 (Abcam; #134401) and anti-Prf1-AlexaFluor488 (BD Biosciences; #563764) primary antibodies after blocking with 5% BSA/PBS for one hour. Phalloidin conjugated with AlexaFluor405 (ThermoFisher Scientific; #A30104) was used to label the CTLs actin cytoskeleton. Fluorescent emission was collected in sequential manner. Post processing of the fluorescence images was performed with ImageJ (National Institute of Health).

dSTORM imaging and analysis

Multicolor dSTORM imaging was performed with primary antibodies directly conjugated with AlexaFluor488 and AlexaFluor647 acquired in sequential manner by using the TIRFM imaging system (Olympus). Antibodies used were anti-Prf1 (BD Biosciences; #563764), anti-Gzmb (BD Biosciences; #560212), anti-TSP-1 (Abcam; #1823) and anti-galectin-1 (ThermoFisher Scientific; #43-7400). $CD8^+$ T-cell released SMAPs were additionally stained with WGA-CF568 (Biotium; #29077-1) or WGA-AlexaFluor647 (ThermoFisher Scientific; #W32466). Fab_2 conjugated secondary antibodies with CF568 (Sigma Aldrich; #SAB4600309) were used to enhance and better resolve the released SMAPs. Firstly, 640-nm laser light was used to excite the AlexaFluor647 dye and switch it to the dark state. Secondly, 488-nm laser light was used to excite the AlexaFluor488 dye and switch it to the dark state. Thirdly, 560-nm laser light was used to excite the CF568 dye and switch it to the dark state. An additional 405-nm laser light was used to reactivate the AlexaFluor647, AlexaFluor488 and CF568 fluorescence. The emitted light from all dyes was collected by the same objective and imaged with an electron-multiplying charge-coupled

device camera at a frame rate of 10 ms per frame. A maximum of 5,000 frames for AlexaFluor647 and AlexaFluor488 and a minimum of 50,000 frames for CF568 were acquired.

As multicolor dSTORM imaging is performed in sequential mode by using three different optical detection paths (same dichroic but different emission filters), an image registration is required to generate the final three-color dSTORM image (*35-37*). Therefore, fiducial markers (TetraSpeck™ Microspheres, ThermoFisher Scientific; #T7279) of 100 nm, which were visible in 488-nm, 561-nm and 640-nm channels, were used to align the 488-nm channel to 640-nm channel. The difference between 561-nm channel and 640-nm channel was negligible and therefore transformation was not performed for 561-nm channel. The images of the beads in both channels were used to calculate a polynomial transformation function that maps the 488-nm channel onto the 640-nm channel, using the MultiStackReg plug-in of ImageJ (National Institute of Health), to account for differences in magnification and rotation, for example. The transformation was applied to each frame of the 488-nm channel. dSTORM images were analyzed and rendered as previously described (*38, 39*) using custom-written software (Insight3, provided by B. Huang, University of California, San Francisco). In brief, peaks in single-molecule images were identified based on a threshold and fit to a simple Gaussian to determine the x and y positions. Only localizations with photon count $\geq$ 2000 photons were included, and localizations that appeared within one pixel in five consecutive frames were merged together and fitted as one localization. The final images were rendered by representing the x and y positions of the localizations as a Gaussian with a width that corresponds to the determined localization precision. Sample drift during acquisition was calculated and subtracted by reconstructing dSTORM images from subsets of frames (500 frames) and correlating these images to a reference frame (the initial time segment). ImageJ was used to merge rendered high-resolution images (National Institute of Health).

Coordinate-based co-localization (CBC) analysis

CBC analysis between TSP-1 and WGA was performed using an algorithm described previously (*40*). To assess the correlation function for each localization, the x-y coordinate list from TSP-1 and WGA dSTORM channels was used. For each localization from the TSP-1 channel, the correlation function to each localization from the WGA channel was calculated. This parameter can vary from −1 (perfectly segregated) to 0 (uncorrelated distributions) to +1 (perfectly co-localized). The correlation coefficients were plotted as a histogram of percentage of occurrences with a 0.1 binning. The percentage of TSP-1 positive signal that colocalizes with WGA signal is the sum of percentages from +0.5 to +1.

Mass Spectrometry

$CD8^+$ T-cell released SMAPs captured on activating or non-activating SLB were lysed with 1x ice-cold lysis buffer (Cell Signaling Technology; #9806S) supplemented with 1x Protease/Phosphatase inhibitor cocktail (Cell Signaling Technology; #5872). Lysates were cleared by centrifugation, digested with trypsin and analyzed on a LC-MS/MS platform consisting of Orbitrap Fusion Lumos coupled to a UPLC ultimate 3000 RSLCnano (ThermoFisher Scientific). Proteomic data was analyzed in Maxquant (V1.5.7.4) and Progenesis QI 4.1 (Waters, ID: Mascot 2.5 (Matrix Science)) using default parameters and Label Free Quantitation. The data was searched against the human Uniprot database (15/10/2014). Only proteins that were detected as distinctive for the activating condition compared to non-activating condition were identified. STRING version 11.0 (https://string-db.org/) database was used to visualize the network plot of the proteins identified specifically in SMAPs released on activating SLB and that were present in at least two from three independent experiments. The list of all identified proteins is available (Data. S1).

Cryo-Soft X-ray Tomography (CSXT)

Carbon coated transmission electron microscopy (TEM) grids (Quantifoil, TAAB Laboratories equipment Ltd,, Reading, UK; #G255) were coated with 0.01% poly-L-lysine (PLL) (Sigma Aldrich; #P8920) for 20 min. After PLL coating the TEM grids were incubated with 2.5 μg/mL of ICAM-1-Fc (R&D Systems, Abingdon, UK; #720-IC) and 5 μg/mL of anti-CD3ε (BioLegend, London, UK; #317302) in PBS for two hours at 37°C, followed by extensive rinse with PBS. $CD8^+$ T-cells were incubated on the TEM grids for two hours and flushed out with ice-cold PBS, and the released SMAPs were immediately plunge-frozen in liquid ethane. Tilt series were collected on the Xradia UltraXRM-S220c X-ray microscope (Zeiss) at the B24 beamline of the Diamond synchrotron with a Pixis-XO:1024B CCD camera (Teledyne Princeton Instruments, Birmingham, UK) and a 40 nm zone plate with X-rays of 500 eV. Tilt series were collected from -70° to +70° with an increment of 0.5°.

X-ray tomograms were reconstructed using etomo part of the IMOD package (*41*). Manual segmentation of the $CD8^+$ T-cell released SMAPs was performed by using the TrakEM2 plugin in ImageJ (National Institute of Health) (*42*).

CRISPR/Cas9 genome editing

Freshly isolated $CD8^+$ T-cells were washed three times in Opti-MEM (Gibco; #11058021). For 1.5 x 10^6 cells, RNP complexes were prepared by mixing trans-activating CRISPR RNA (Alt-R Cas9 tracrRNA) and target-specific CRISPR-Cas9 gRNA for TSP-1 (IDT; Hs.Cas9.THBS1.1.AC; sequence: GTCTTCAGCGTGGTGTCCAA) or galectin-1 (IDT; Hs.Cas9.LGALS1.1.AA; sequence: CGCACTCGAAGGCACTCTCC) in equimolar amounts (200 pmol) prior to incubation at 95˚C for 5 min. 150 pmol of Alt-R S.p. Cas9 Nuclease V3 (IDT, Leuven, BE; #1081058) and

the duplexed gRNA were mixed in IDT nuclease-free duplex buffer and assembled for 15 min at 37˚C. Alt-R Cas9 Electroporation Enhancer (IDT, Leuven, BD; #1075915) (200 pmol) was added to the resultant RNP complexes and mixed with the cells in 50 μL of Opti-MEM prior to electroporation in an ECM 880 Square Wave Electroporator (BTX Harvard Apparatus, Cambourne, UK). The cells were expanded with anti-CD3/anti-CD28 T-cell activation and expansion beads for 3 days in complete R10 medium supplemented with 50 Units/mL of IL-2. After three days of incubation the beads were removed, and the cells were seeded with 35 Units/mL of IL-2 in complete R10 medium at 10^6 cells/mL for further two days. The activated and rested cytotoxic $CD8^+$ T-cells were used next day. Immuno-blotting was used to assess the percentage of protein reduction compared to the control condition without the specific gRNA.

LDH cytotoxicity assay

$CD8^+$ T-cells were plated onto activating or non-activating SLB with increased amounts of anti-CD3ε-Fab (30, 300 and 3000 molecules/μm^2) for 90 min at 37°C. After incubation, the cells were flushed out with ice-cold PBS and the released SMAPs captured on SLB were incubated for further four hours with target cells (CHO). After incubation, the supernatant was collected, spun down to remove cells and cell debris, and used to assess the cytotoxicity levels by measuring the amount of released lactate dehydrogenase (LDH) following the manufacturer's protocol (TaKaRa Bio, Saint-Germain-en-Laye, FR; #MK401). For cell-cell mediated cytotoxicity assays, 5 x 10^6 target cells (K562) were pulsed with 10 μg/mL of anti-CD3ε (BioLegend; #317326) for 1 hour at 4 °C. After washing out the unbound anti-CD3ε, target cells were incubated with $CD8^+$ T-cell blasts, or with TSP-1 or galectin-1 knockout $CD8^+$ T-cells at 1:1 ratio for 2 hours at 37 °C. After incubation, cells were spun down and the cytotoxicity levels were quantified by measuring the amount of

released LDH in the supernatant following the manufacturer's protocol. Data were normalized to the control condition ($CD8^+$ T-cell blasts).

Enzyme-Linked Immunosorbent Assay (ELISA)

$CD8^+$ T-cells were plated onto activating or non-activating SLB for 90 min at 37°C. After incubation, supernatants were recovered, and cells were removed with ice-cold PBS. $CD8^+$ T-cell released SMAPs were rinsed twice in ice-cold PBS and disrupted with 1x ice-cold lysis buffer (Cell Signaling Technology; #9806S) supplemented with 1x Protease/Phosphatase inhibitor cocktail (Cell Signaling Technology, London, UK; #5872). Cell supernatants and $CD8^+$ T-cell released SMAPs lysates were cleared by centrifugation. TSP-1, Prf1 and Gzmb presence was quantified by sandwich ELISA (Abcam; ab193716; ab46068; ab235635; respectively), according to manufacturer's instructions. Absorbance was measured at 450 nm.

Immuno-blotting

$CD8^+$ T-cells were plated onto activating or non-activating SLB for 90 min at 37°C. After incubation and cell removal with ice-cold PBS, the $CD8^+$ T-cell released SMAPs were rinsed twice in ice-cold PBS and disrupted with 1x ice-cold lysis buffer (Cell Signaling Technology; #9806S) supplemented with 1x Protease/Phosphatase inhibitor cocktail (Cell Signaling Technology; #5872). Lysates were cleared by centrifugation and reduced in protein sample loading buffer (Li-Cor; #928-40004), resolved by 4-15% Mini-PROTEAN SDS-PAGE gel (Bio-Rad; #4561084), transferred to nitrocellulose membrane, and immuno-blotted with anti-Gzmb (Cell Signaling Technology; #4275S), anti-CD45 (Cell Signaling Technology; #13917S), anti-LAMP-1 (Cell Signaling Technology; #9091S), anti-β2-Integrin (Cell Signaling Technology; #73663S), anti-

TSP-1 (ThermoFisher Scientific; #MA5-11330), anti-galectin-1 (Cell Signaling Technology; #12936) and anti-Prf1 (Abcam; #Ab97305) antibodies. Immuno-blotting analysis of TSP-1 in whole cell lysates of $CD8^+$ T-cells, primary NK cells and primary CTLs, under reducing or non-reducing conditions, was performed with anti-TSP-1 antibodies binding to different epitopes of TSP-1 (Abcam; #263952; Cell Signaling Technology; #37879s; ThermoFisher Scientific; #MA5-11330, #MA5-13390). Purified full-length human TSP-1 protein isolated from platelets (Sigma Aldrich; #605225-25UG) was used as a control. Near-Infrared Western Blot Quantitative Detection was performed using the Odyssey CLx system (Li-Cor, Lincoln, NE) and the images were quantified using the Image Studio Lite software.

Statistical analysis

Samples were tested for normality with a Kolmogorov–Smirnov test. The statistical significance for multiple comparisons was assessed with one-way analysis of variance (ANOVA) with Tukey's post hoc test. All statistical analyses were performed with OriginPro 9.1 (OriginLab, Northampton, MA) analysis software.

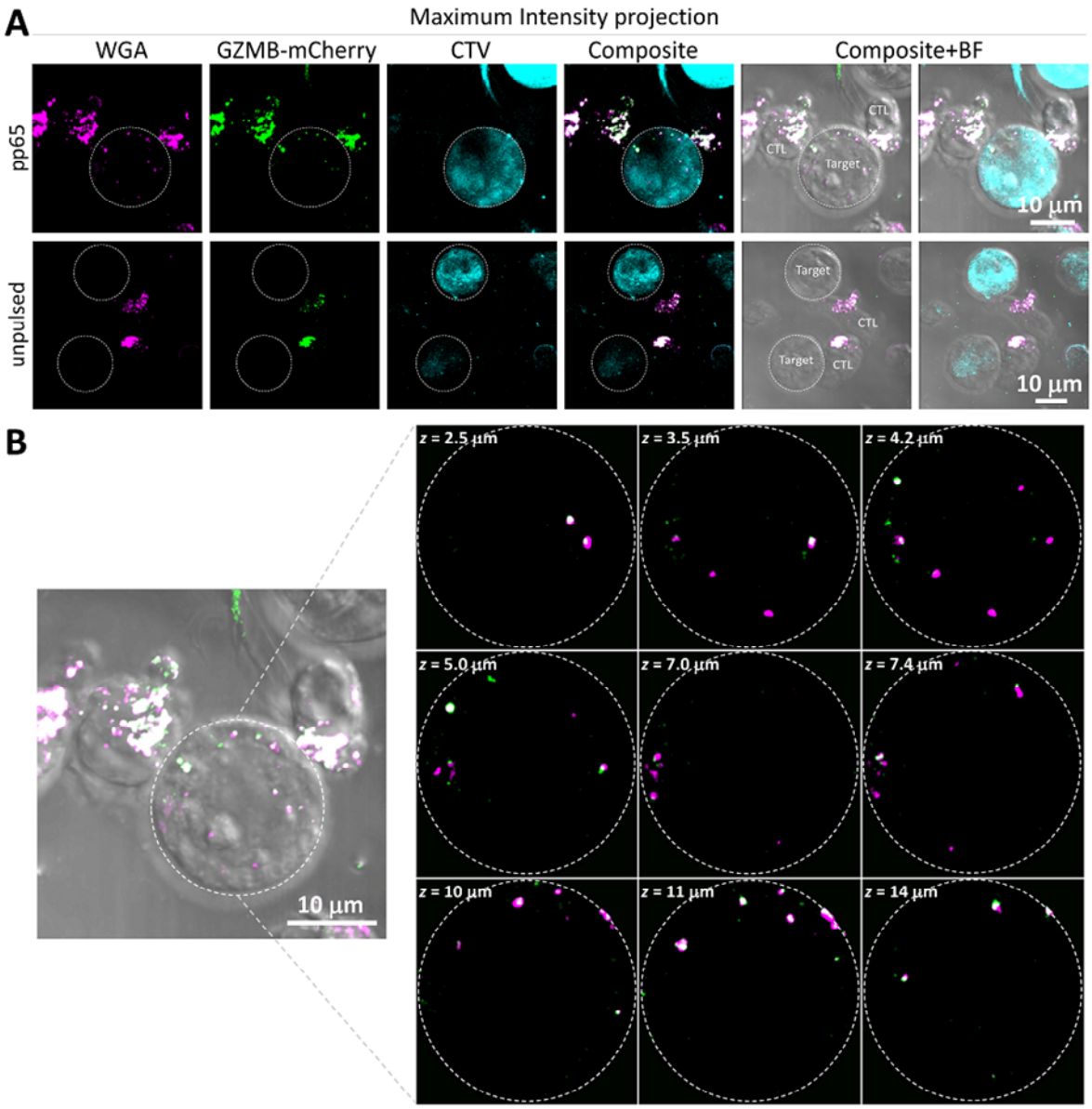

Fig. S1.

Transfer of Gzmb-mCherry$^+$ SMAPs from antigen-specific CTLs to target cells. Maximum intensity projection of confocal *z*-stack images depicting the transfer of Gzmb-mCherry$^+$ (green) and WGA (magenta) labeled SMAPs from an antigen-specific CTL clone into pp65-pulsed JY target cells (A, top row). CTLs were also incubated with unpulsed JY target cells (A, bottom row). Target cells were labeled with CTV and are highlighted by dashed circles (Target). BF, bright field

microscopy. Scale bar, 10 μm. (B) 3D z stack mosaic demonstrating the presence of SMAPs at different z planes from the pp65-pulsed target cell in panel A. SMAPs were labelled with Gzmb-mCherry^{+} (green) and WGA (magenta). A dashed circle demarcates the target cell. Scale bar, 10 μm.

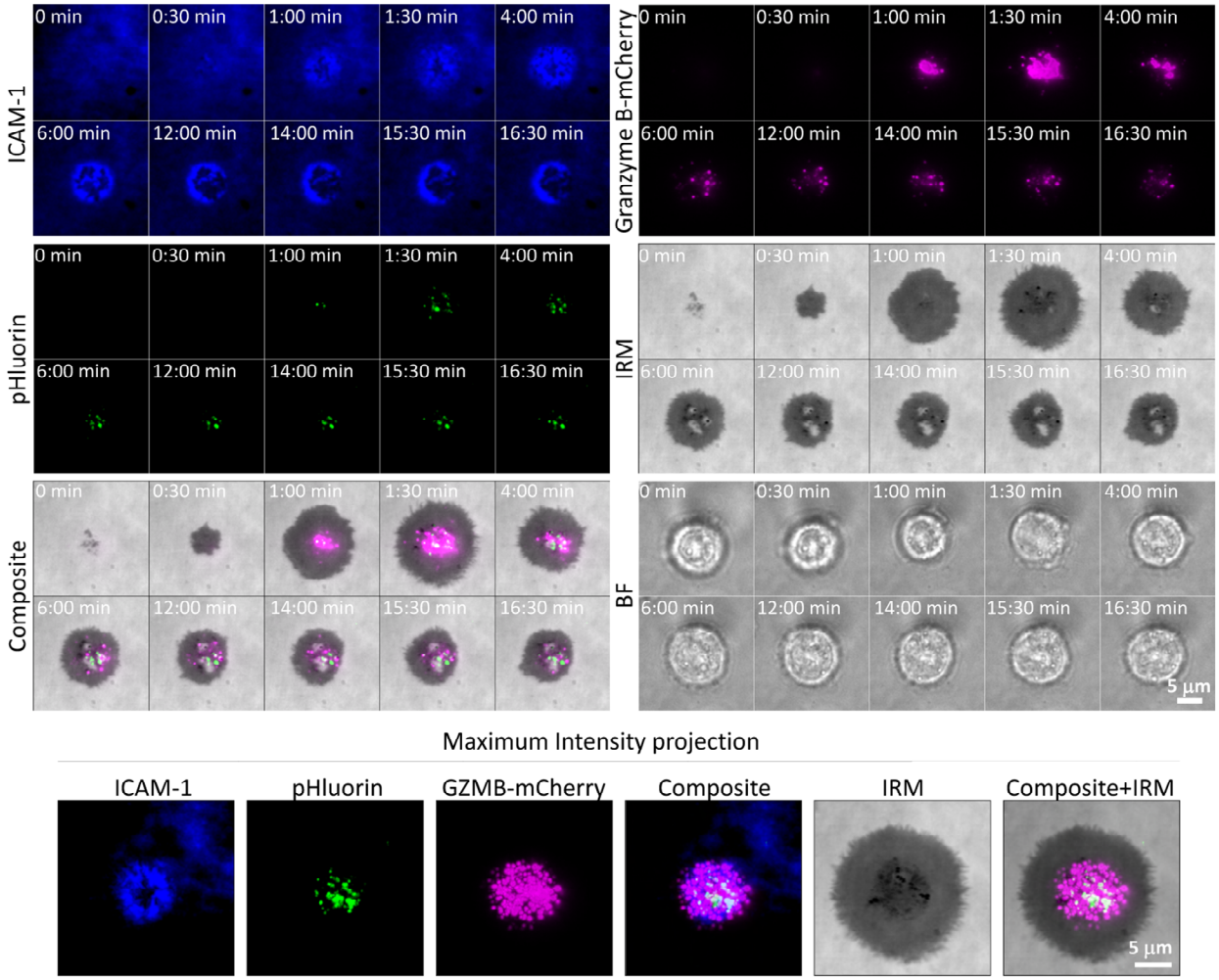

Fig. S2.

Live imaging of the release of SMAPs by Gzmb-mCherry-SEpHluorin transfected CD8$^+$ T-cells. CD8$^+$ T-cells transfected with Gzmb-mCherry-SEpHluorin (magenta/green) were incubated on activating (ICAM-1 + anti-CD3ε) SLB and imaged live by TIRFM. Snapshots of different time points are shown. The formation of a mature IS is indicated by an ICAM-1 ring (blue). Maximum intensity projection of the time lapse (bottom row). Interference reflection microscopy (IRM) and composite images are shown. BF, bright field microscopy. Scale bar, 5 µm.

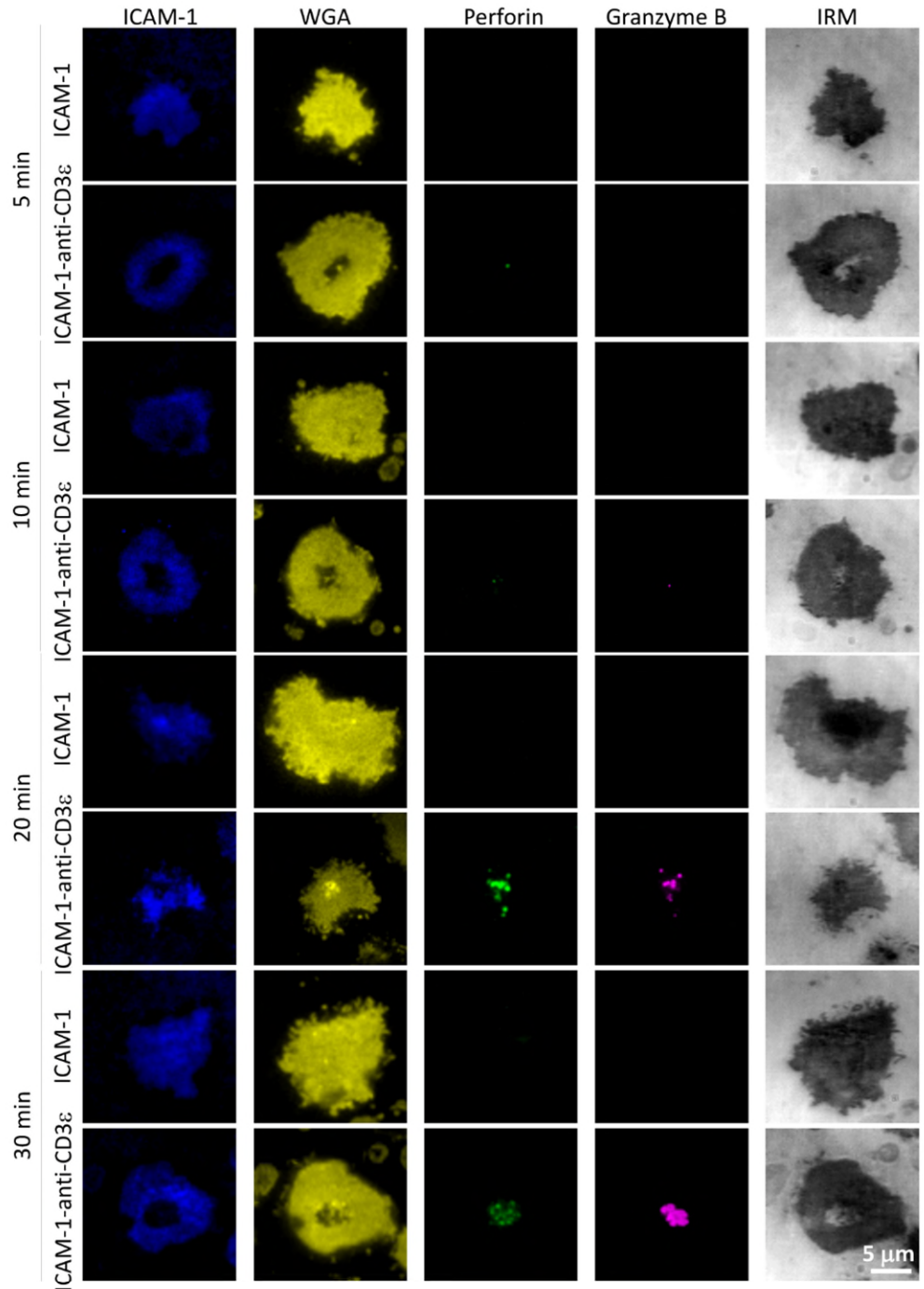

Fig. S3.

Time-dependent release of Prf1$^+$ and Gzmb$^+$ SMAPs at the IS. TIRFM images of CD8$^+$ T-cells incubated for the indicated times on non-activating (ICAM-1) or activating (ICAM-1 + anti-CD3ε)

SLB in the presence of anti-Prf1 (green) and anti-Gzmb (magenta) antibodies. After fixation, cells were stained with WGA (yellow) to visualize the cell membrane. The formation of a mature IS is indicated by an ICAM-1 ring (blue). IRM, interference reflection microscopy. Scale bar, 5 μm.

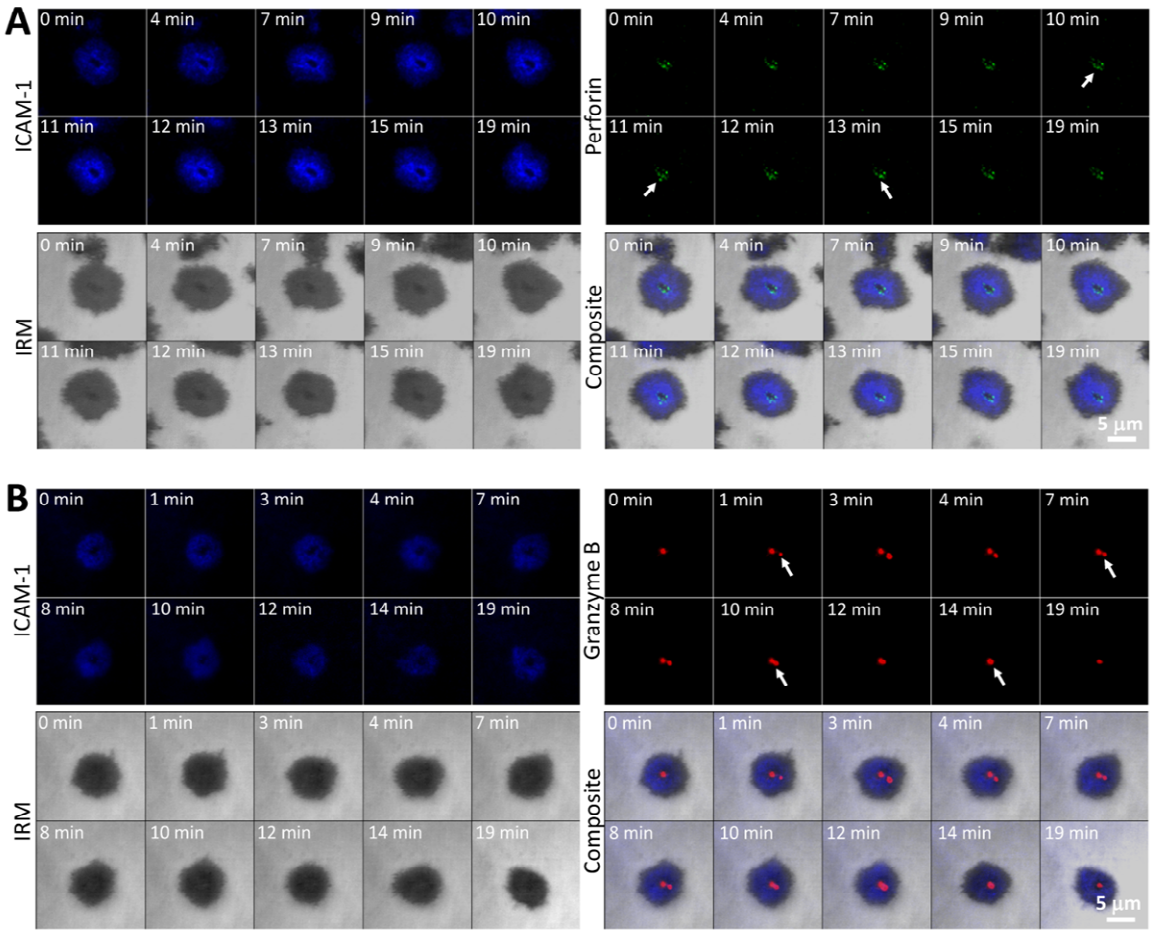
A
ICAM-1
Perforin
IRM
Composite
0 min
4 min
7 min
9 min
10 min
11 min
12 min
13 min
15 min
19 min
5 µm
B
ICAM-1
Granzyme B
IRM
Composite
0 min
1 min
3 min
4 min
7 min
8 min
10 min
12 min
14 min
19 min
5 µm

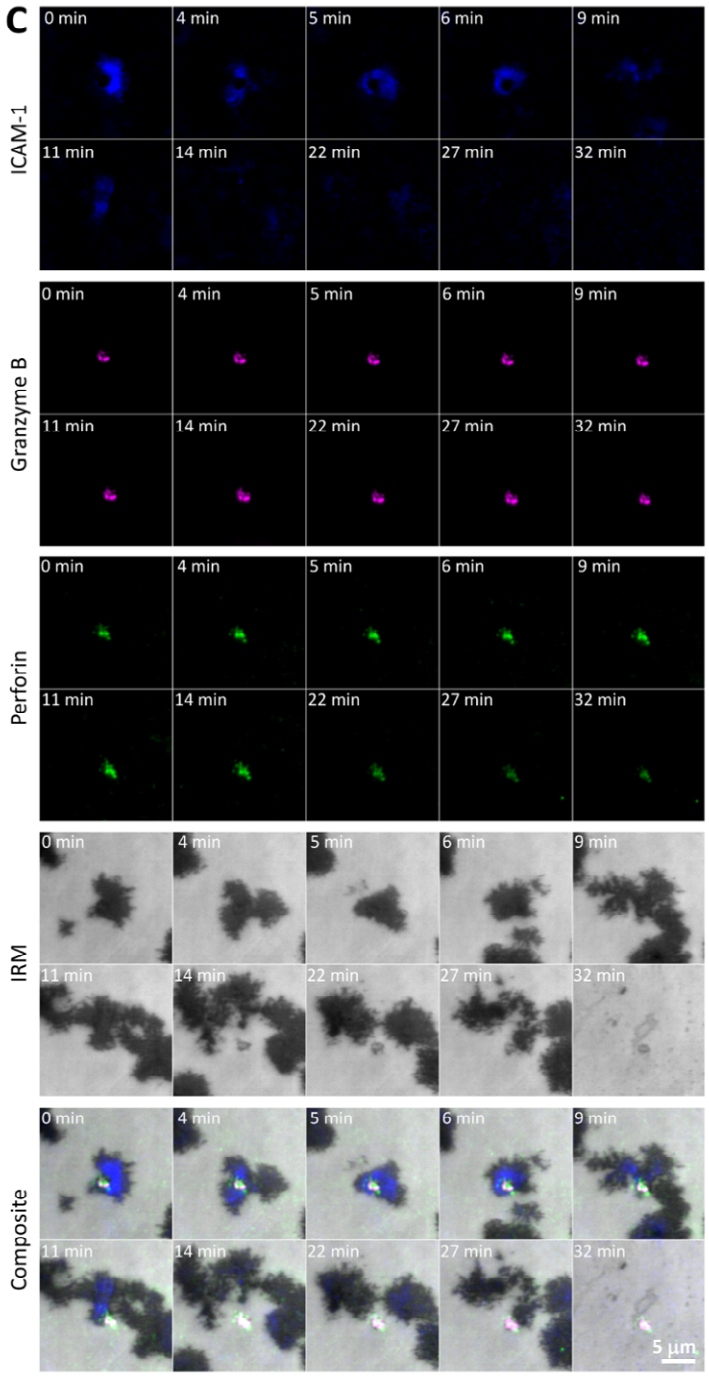

Fig. S4.

Live imaging of the release of Prf1$^+$ and Gzmb$^+$ SMAPs by CD8$^+$ T-cells. CD8$^+$ T-cells were incubated on activating (ICAM-1 + anti-CD3ε) SLB in the presence of anti-Prf1 (A, green), anti-

Gzmb (B, red) or both (C) antibodies and imaged live by TIRFM for 50 minutes. Snapshots of different time points are shown. Time zero refers to the start of imaging after CTLs have had 20 min to interact with SLB. The formation of a mature IS is indicated by an ICAM-1 ring (blue). Arrows indicate the presence of SMAPs. Interference reflection microscopy (IRM) and composite images are shown. Scale bar, 5 μm.

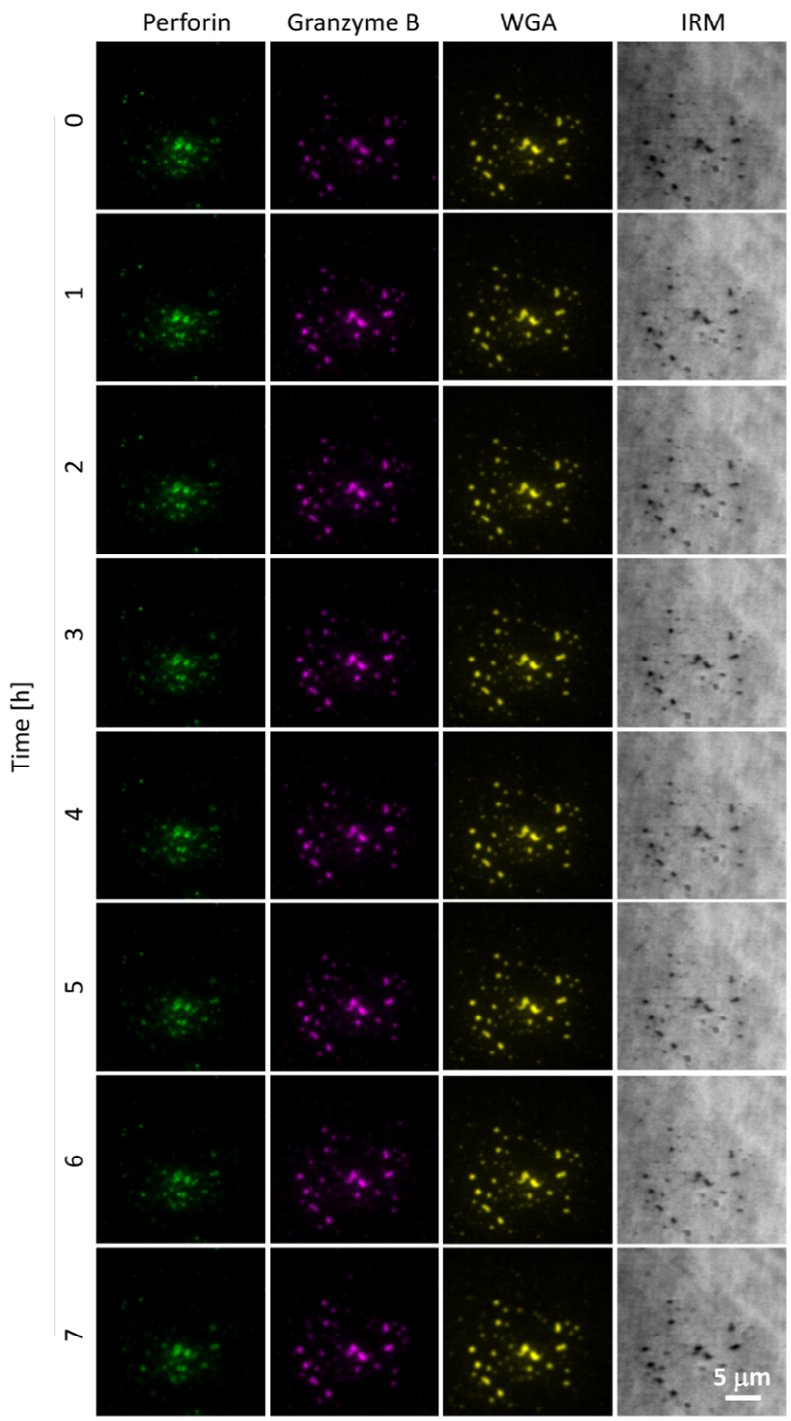

Fig. S5.

Prf1 and Gzmb were components of SMAPs released by CD8$^+$ T-cells. TIRFM images of CD8$^+$ T-cell released SMAPs captured on activating (ICAM-1 + anti-CD3ε) SLB over a time course of

seven hours. Images of the same area were taken every hour. Time zero refers to the start of imaging after SMAPs release and $CD8^+$ T-cell removal. SMAPs were labeled with anti-Prf1 (green) and anti-Gzmb (magenta) antibodies, and with WGA (yellow). IRM, interference reflection microscopy. Scale bar, 5 μm.

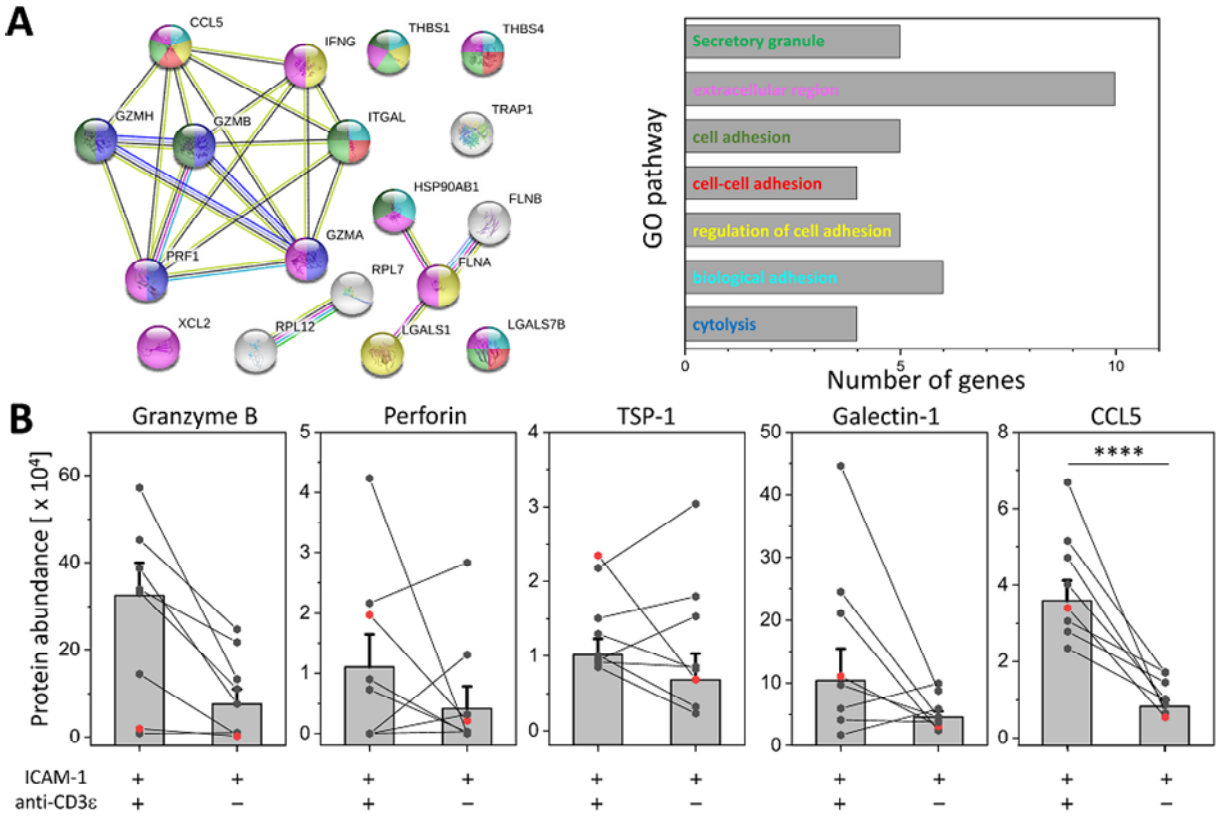

C

Granzyme B OS=Homo sapiens GN=GZMB PE=1 SV=2

Database:	SwissProt
Score:	151
Nominal mass (M_r):	28097
Calculated pI:	9.62
Taxonomy:	Homo sapiens

Sequence similarity is available as an NCBI BLAST search of P10144 against nr.

Search parameters

MS data file:	MSQ1171.mgf
Enzyme:	Trypsin: cuts C-term side of KR unless next residue is P.
Fixed modifications:	Carbamidomethyl (C)
Variable modifications:	Deamidated (N), Deamidated (Q), Oxidation (M)

Protein sequence coverage: 29%

Matched peptides shown in ***bold red***.

```
  1 MQPILLLLAF LILPRADAGE IIGGHEAKPH SRPYMAYLMI WDQKSLKRCG
 51 GFLIRDDFVL TAAHCWGSSI NVTLGAHNIK EQEPTQQFIP VKRPIPHPAY
101 NPKNFSNDIM LLQLERKAKR TRAVQPLRLP SNKAQVKPGQ TCSVAGWGQT
151 APLGKHSHTL QEVKMTVQED RKCESDLRHY YDSTIELCVG DPEIKKTSFK
201 GDSGGPLVCN KVAQGIVSYG RNNGMPPRAC TKVSSFVHWI KKTMKRY
```

Galectin-1 OS=Homo sapiens GN=LGALS1 PE=1 SV=2

Database:	SwissProt
Score:	293
Nominal mass (M_r):	15048
Calculated pI:	5.34
Taxonomy:	Homo sapiens

Sequence similarity is available as an NCBI BLAST search of P09382 against nr.

Search parameters

MS data file:	MSQ1171.mgf
Enzyme:	Trypsin: cuts C-term side of KR unless next residue is P.
Fixed modifications:	Carbamidomethyl (C)
Variable modifications:	Deamidated (N), Deamidated (Q), Oxidation (M)

Protein sequence coverage: 51%

Matched peptides shown in ***bold red***.

```
  1 MACSLVASNL NLKPGSCLRV RGEVASDAKS FVLHLGKDSN NLCLEFKPRE
 51 NAHGDANTIV CNSKDGGAWG TEQREAVFPF QPGSVAEVCI TFDQANLTVK
101 LPDGYEFKFP NRLNLEAINY MAADGDFKIK CVAFD
```

Perforin-1 OS=Homo sapiens GN=PRF1 PE=1 SV=1

Database:	SwissProt
Score:	39
Nominal mass (M_r):	62479
Calculated pI:	8.05
Taxonomy:	Homo sapiens

Sequence similarity is available as an NCBI BLAST search of P14222 against nr.

Search parameters

MS data file:	MSQ1171.mgf
Enzyme:	Trypsin: cuts C-term side of KR unless next residue is P.
Fixed modifications:	Carbamidomethyl (C)
Variable modifications:	Deamidated (N), Deamidated (Q), Oxidation (M)

Protein sequence coverage: 2%

Matched peptides shown in ***bold red***.

```
  1 MAARLLLLGI LLLLLPLPVP APCHTAARSE CKRSNKFVFR AMLASESVDV
 51 TSLRRSGSSF VDTQRFLRFD STCTLCEHAL QESTLQRLPL ALTNMRAQDS
101 GCQRNVTRAK VSSTEAVARD AARSINDMK VSLDVTPKPT SNVNVSVAGS
151 HSQAAHFAAQ KTHQDQVSFS TDFVERFVS FWVVNTPPLN PDFPRALGDL
201 PRHFNASTQP AVLRLISNVG THFIRAVELG GRISALTALR TCELALEGLT
251 DNEVEDCLTV EAQVNIGIHG SISAEARACE EKKKKHKMTA SFHQTYRERH
301 SEVVSSHHIS INDLLFSIQA QPEQYSAMVN SLPSSFGLVD VTLEPLHVLL
351 DSQDPRREAL RRALSQVLTD RARMRDCSRP CPPSRQKSPR DPCQQVCHGS
401 AVTTDDCCFR QRSLAQLEVT FQAMSLNGD WTTATDAIVK LFFSQELRI
451 STVMDNGNPI MSVNLDFDDV LLATDGFLRL QVWGQCDSNR DDLLSTCDQA
501 PFSSSHEVRC NLHNHSHLKFR YHARCLPNLG GSTCLDVPQ MLGEPPGHR
551 SGAVM
```

C-C motif chemokine 5 OS=Homo sapiens GN=CCL5 PE=1 SV=3

Database:	SwissProt
Score:	102
Nominal mass (M_r):	10268
Calculated pI:	9.27
Taxonomy:	Homo sapiens

Sequence similarity is available as an NCBI BLAST search of P13501 against nr.

Search parameters

MS data file:	MSQ1171.mgf
Enzyme:	Trypsin: cuts C-term side of KR unless next residue is P.
Fixed modifications:	Carbamidomethyl (C)
Variable modifications:	Deamidated (N), Deamidated (Q), Oxidation (M)

Protein sequence coverage: 26%

Matched peptides shown in ***bold red***.

```
  1 MKVSAAALAV ILIATALCAP ASASPYSSDT TPCCFAYIAR PLPRAHIKEY
 51 FYTSGKCSNP AVVFVTRKNR QVCANPEKKW VREYINSLEM S
```

Thrombospondin-1 OS=Homo sapiens GN=THBS1 PE=1 SV=2

Database:	SwissProt
Score:	253
Nominal mass (M_r):	133291
Calculated pI:	4.71
Taxonomy:	Homo sapiens

Sequence similarity is available as an NCBI BLAST search of P07996 against nr.

Search parameters

MS data file:	MSQ1171.mgf
Enzyme:	Trypsin: cuts C-term side of KR unless next residue is P.
Fixed modifications:	Carbamidomethyl (C)
Variable modifications:	Deamidated (N), Deamidated (Q), Oxidation (M)

Protein sequence coverage: 7%

Matched peptides shown in ***bold red***.

```
  1 MGLAWGLGVL FLMHVCGTNR IPESGGDNSV FDIFELTGAA RKGSGRRLVK
 51 GPDPSSPAFR IEDANLIPPV PDDKFQDLVD AVRAEKGFLL LASLRQMKKT
101 RGTLLALERK DHSGQVFSVV SNGKAGTLDL SLTVQGKQHV VSVEEALLAT
151 GQWKSITLFV QEDRAQLYID CEKMENAELD VPIQSVFTRD LASIARLRIA
201 KGGVNDNFQG VLQNVRFVFG TTPEDILRNK GCSSSTSVLL TLDNNVVNGS
251 SPAIRTNYIG HKTKDLQAIC GISCDELSSM VLELRGLRTI VTTLQDSIRK
301 VTEENKELAN ELRRPPLCYN PGVQYVERDN EWVDSCTECR CQNSVTICKK
351 VSCPIMPCSN ATVPDGECCP RCWPSDSADD GWSPWSEWTS CSTSCGNGIQ
401 QRGRSCDSLN NRCEGSSVQT RTCHIQECDK RFKQDGGWSH WSPWSSCSVT
451 CGDGVITRIR LCNSPSPQMN GKPCEGEARE IKACKKDACP IHGGWSPWSP
501 WDICSVTCGG GVQKRSRLCN NPTPQFGGKD CVGDVTENQI CNKQDCPIDG
551 CLSNPCFAGV KCTSVPDGSW KCGACPPGYS GNGIQCTDVD ECKEVPDACF
601 NHNGEHHCEN TDPGYNCLPC PPRFTGSQPF GQGVEHAIAN KQVCKPRNPC
651 TDGTHDCNKN AKCNYLGHYS DPMYRCECKP GYAGNGIICG EDTDLDGWPN
701 ENLVCVANAT YHCKKDNCPN LPNSGQEDYD KDGIGDACDD DDDNDKIPDD
751 RDNCPFHYNP AQYDYDRDDV GDRCDNCPYH HNPDQADTDN NGEGDACAAD
801 IDGDGILNER DNCQYVYNVD QRDTDMDGVG DQCDNCPLEH NPDQLDSDSD
851 RIGDTCDNNQ DIDEDGHQNN LDNCPYVPNA NQADHDKDGK GDACDHDDDN
901 DGIPDDKDNC RLVPNPDQKD SDGDGRGDAC KDDFDHDSVP DIDDICPENV
951 DISETDFRRF QMIPLDPKGT SQNDPNWVVR HQGKELVQTV NCDPGLAVGY
1001 DEFNAVDFSG TFFINTERDD DYAGFVFGYQ SSSRFYVVMW KQVTQSYWDT
1051 NPTRAQGYSG LSVKVVNSTT GPGEHLRNAL WHTGNTPGQV RTLWKDPRHI
1101 GWKDFTAYRW RLSHRPKTGF IRVVMYEGKK IMADSGPIYD KTYAGGRLGL
1151 FVFSQEMVFF SDLKYECRDP
```

Fig. S6.

Protein abundance of major proteins identified by mass spectrometry in $CD8^+$ T-cell released SMAPs. (A) Network plot and GO pathway of the proteins identified specifically in SMAPs released on activating SLB. (B) Protein abundance of five major proteins detected in SMAPs released from $CD8^+$ T-cells on non-activating (ICAM-1) or activating (ICAM-1 + anti-CD3ε) SLB. Each dot represents one donor. The red color dot marks the donor that was used as an example in Figure 2B. Horizontal lines and error bars represent mean ± SEM. (C) Peptides detected in proteomics analysis with 1% FDR and score cut-off of 20 for proteins in (B). The peptides sequence is highlighted in red. ****, $p < 0.0001$. Not significant differences are not shown.

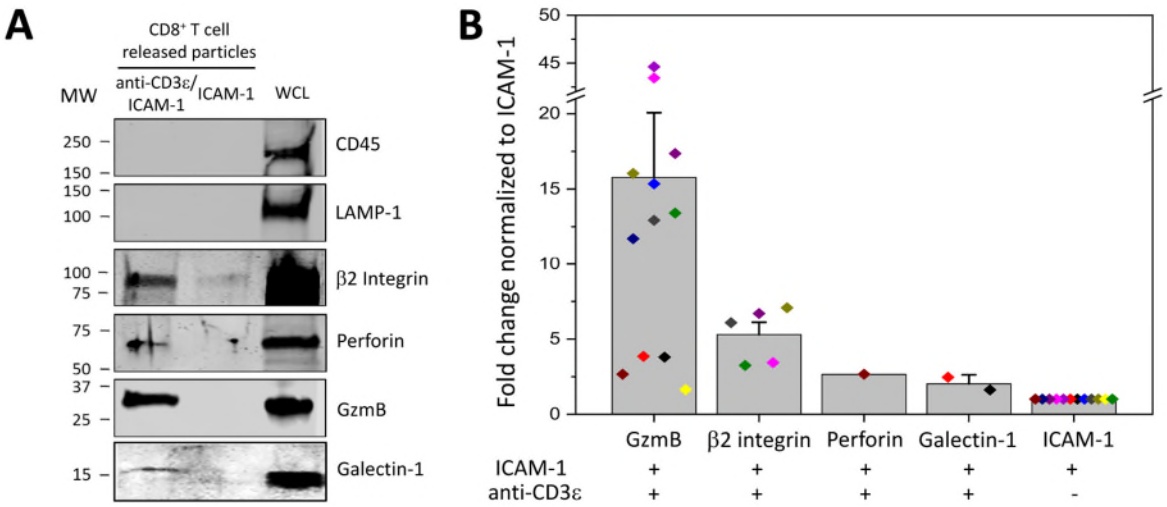

Fig. S7.

Detection of Prf1, Gzmb and β2-integrin on CD8⁺ T-cell released SMAPs by immuno-blotting. (A) SMAPs released on non-activating (ICAM-1) or activating (ICAM-1 + anti-CD3ε) SLB were lysed and analyzed by immuno-blotting with the indicated antibodies (right of panels). Whole cell lysates (WCL) were analyzed in parallel and control for the absence of contamination with cellular membranes. MW, molecular weight (left of panels). (B) Quantification of the expression of components of SMAPs from immuno-blot data. Each colored dot represents one donor. Horizontal lines and error bars represent mean ± SEM.

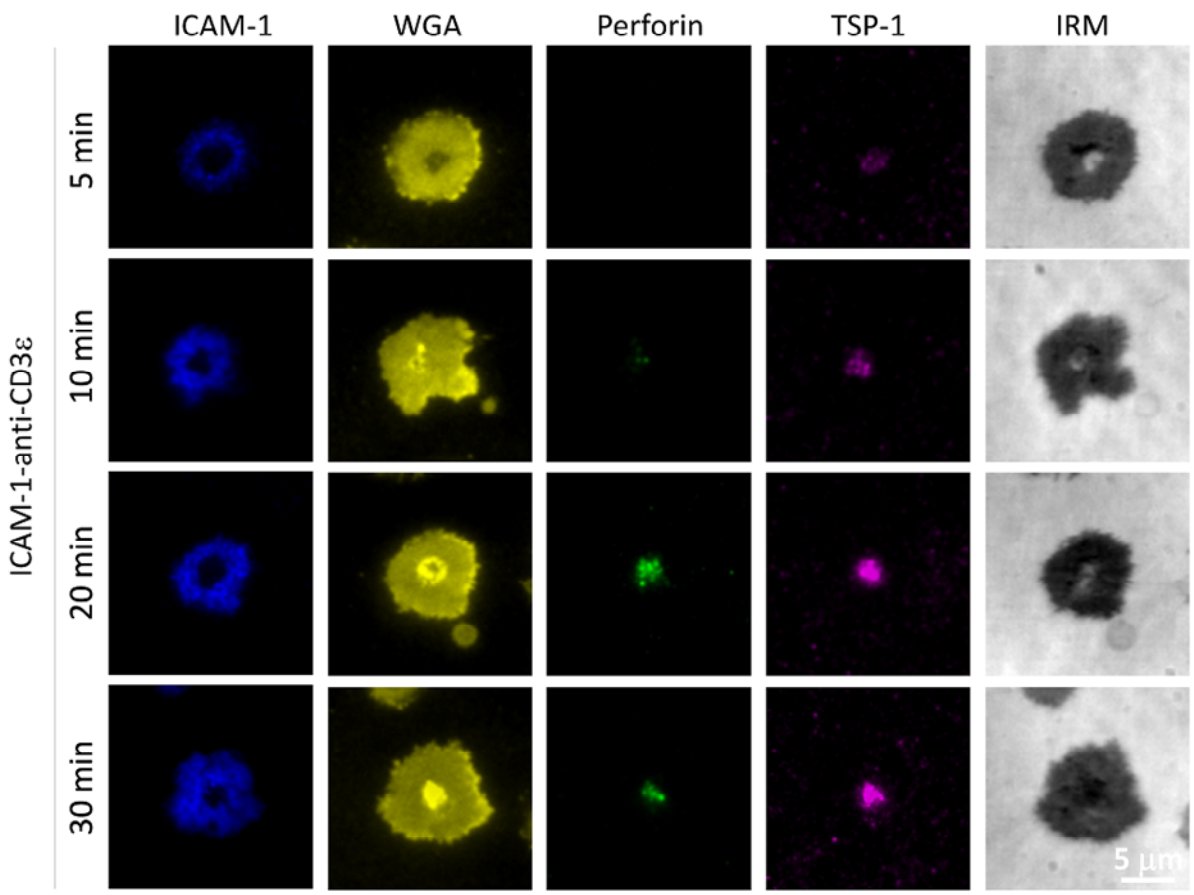

Fig. S8.

TSP-1 containing SMAPs were released at the IS and co-localized with Prf1. TIRFM images of $CD8^+$ T-cells incubated for the indicated times on activating (ICAM-1 + anti-CD3ε) SLB in the presence of anti-Prf1 (green) and anti-TSP-1 (magenta) antibodies. After fixation, cells were stained with WGA (yellow) to visualize the cell membrane. The formation of a mature IS is indicated by an ICAM-1 ring (blue). IRM, interference reflection microscopy. Scale bar, 5 µm.

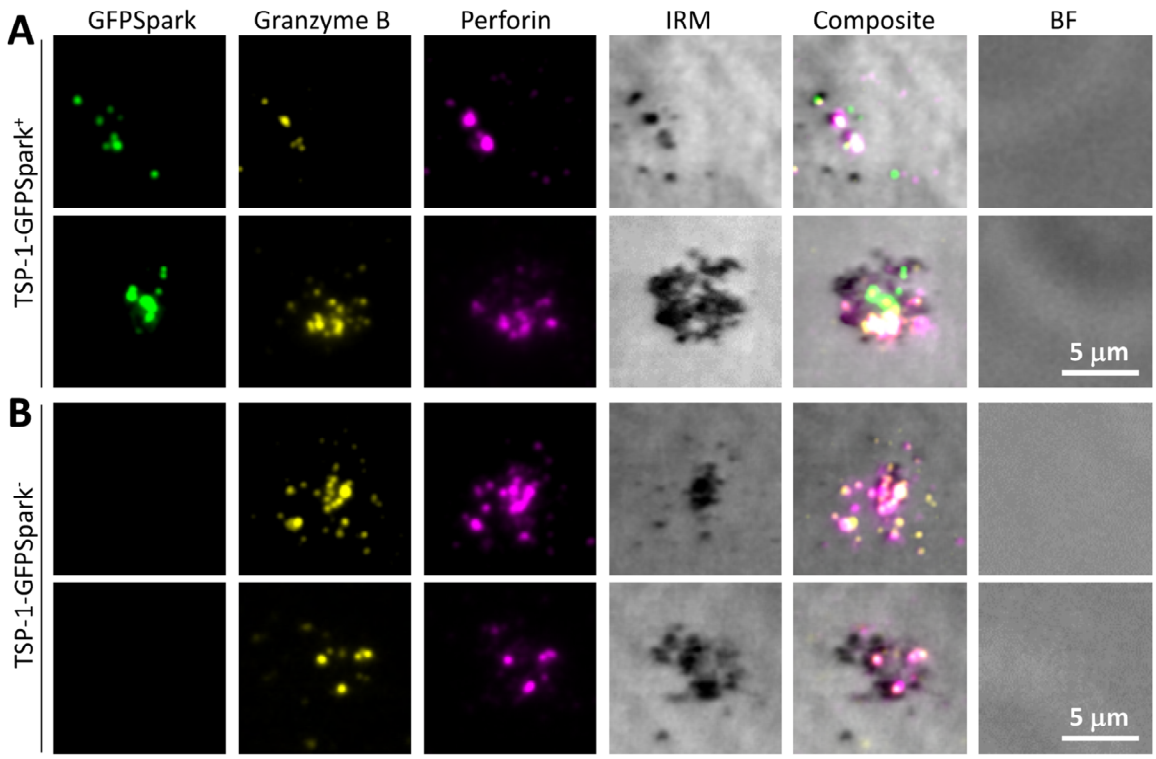

Fig. S9.

TSP-1-GFPSpark transfected CD8$^+$ T-cells released GFP$^+$ SMAPs. (A) TIRFM images of TSP-1-GFP$^+$ SMAPs (green) released from CD8$^+$ T-cells transfected with TSP-1-GFPSpark. Released SMAPs were further stained with anti-Gzmb (yellow) and anti-Prf1 (magenta) antibodies. (B) SMAPs released from non-transfected CD8$^+$ T-cells lacked GFP signal but were still positive for Gzmb (yellow) and Prf1 (magenta). IRM, interference reflection microscopy. BF, bright field microscopy. Scale bar, 5 μm.

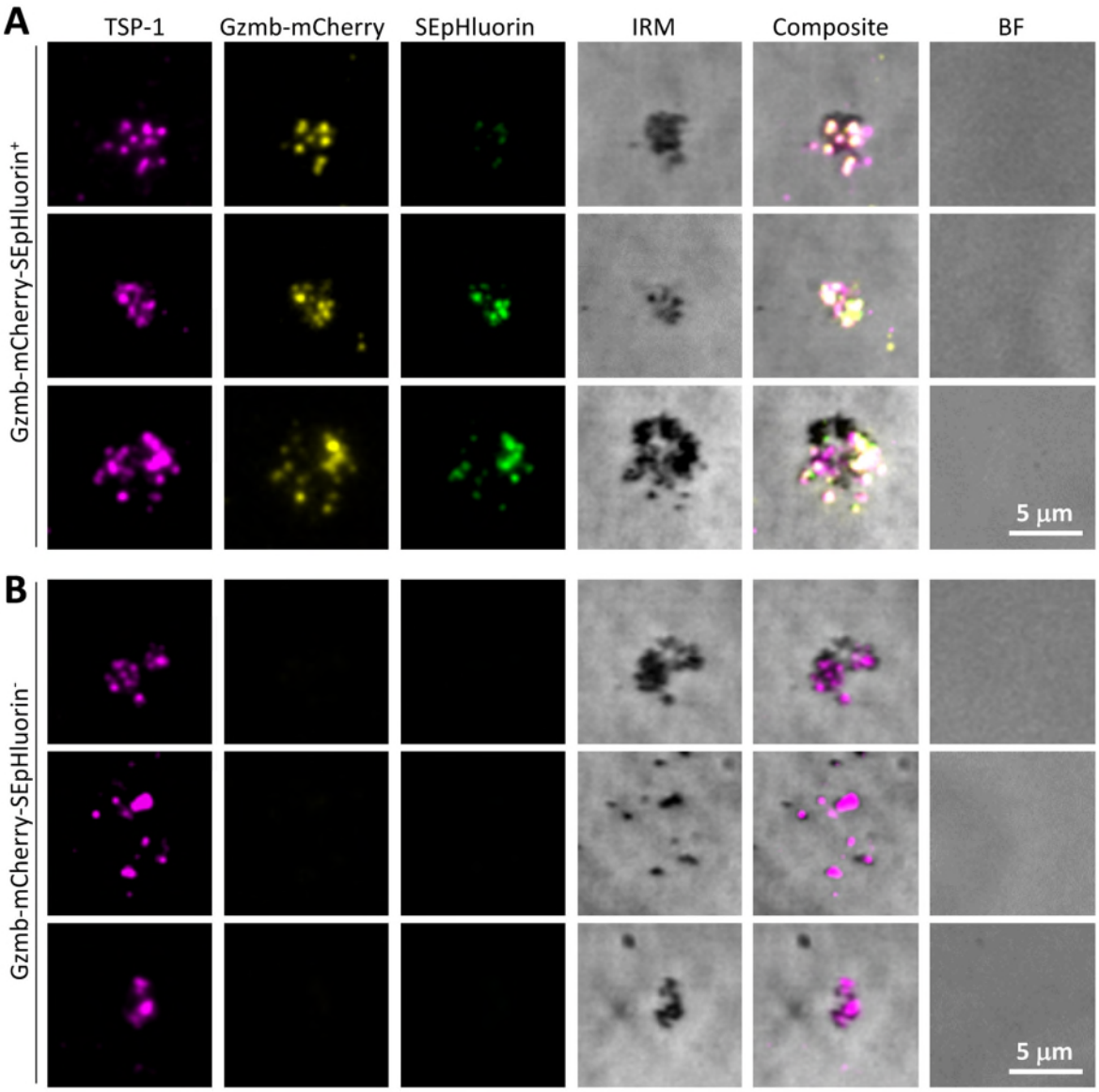

Fig. S10.

Gzmb-mCherry-SEpHluorin transfected CD8$^+$ T-cells released TSP-1$^+$ SMAPs. (A) TIRFM images of Gzmb$^+$ SMAPs (yellow/green) released from CD8$^+$ T-cells transfected with Gzmb-mCherry-SEpHluorin. Released SMAPs were further stained with anti-TSP-1 (magenta) antibody. (B) SMAPs released from non-transfected CD8$^+$ T-cells lacked mCherry and pHluorin signals but were still positive for TSP-1 (magenta). IRM, interference reflection microscopy. BF, bright field microscopy. Scale bar, 5 μm.

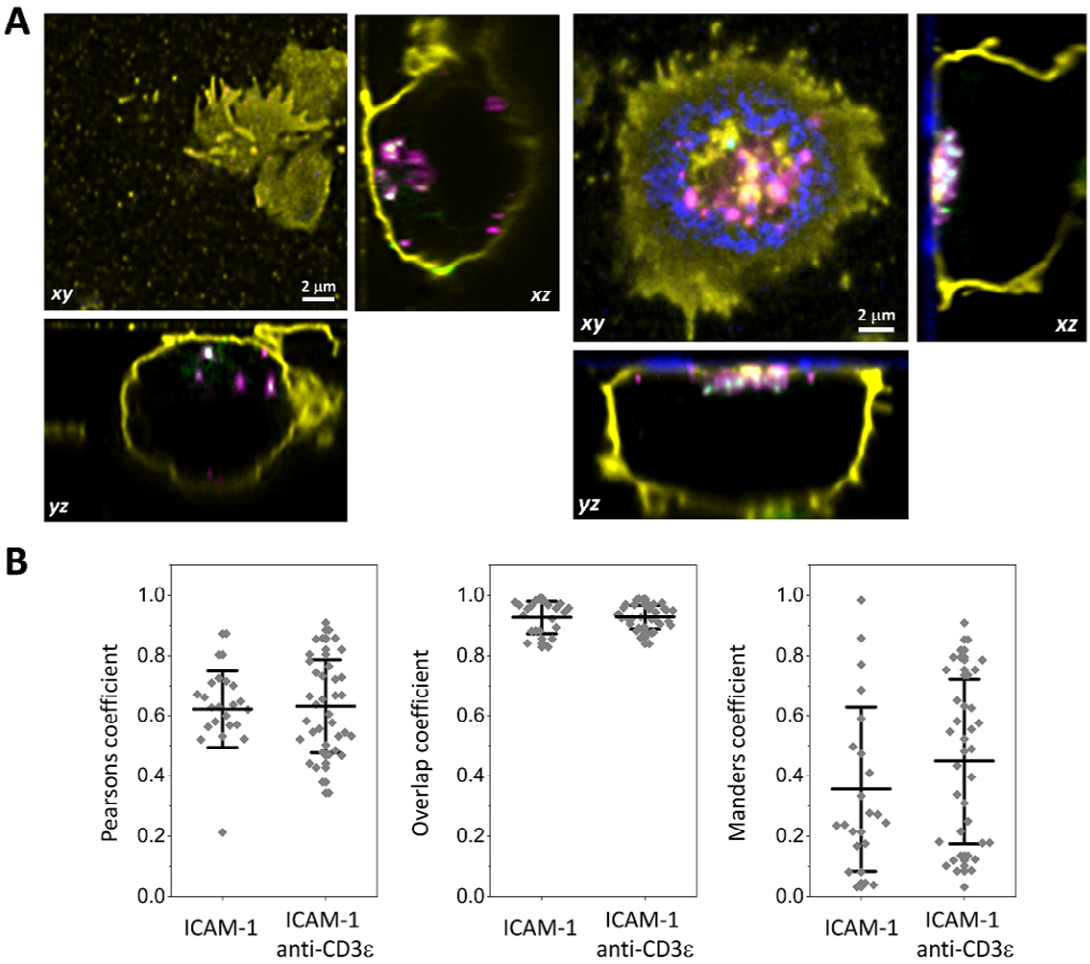

Fig. S11.

Gzmb and TSP-1 were already associated in SMAPs in non-activating conditions. (A) 3D confocal *z*-stack projection and orthogonal views of $CD8^+$ T cells co-transfected with Gzmb-mCherry-SEpHluorin (magenta) and TSP-1-GFPSpark (green) on non-activating (ICAM-1; left) or activating (ICAM-1 + anti-CD3ε; right) SLB. pHluorin is non-fluorescent in the secretory lysosomes. Thus, co-localization between GFPSpark and mCherry signals represents TSP-1 and Gzmb. Cells were fixed and stained with WGA (yellow) to visualize the cell membrane. The formation of a mature IS is indicated by an ICAM-1 ring (blue). Scale bar, 2 µm. (B) Quantification of the colocalization between Gzmb and TSP-1 staining in non-activating (ICAM-1) and activating (ICAM-1 + anti-CD3ε) conditions assessed by Pearsons coefficient (left), Overlap coefficient

(middle) and Manders coefficient (right). Each dot represents one cell. Horizontal line and error bar represent mean ± SD; n=1 donor. Not significant differences are not shown.

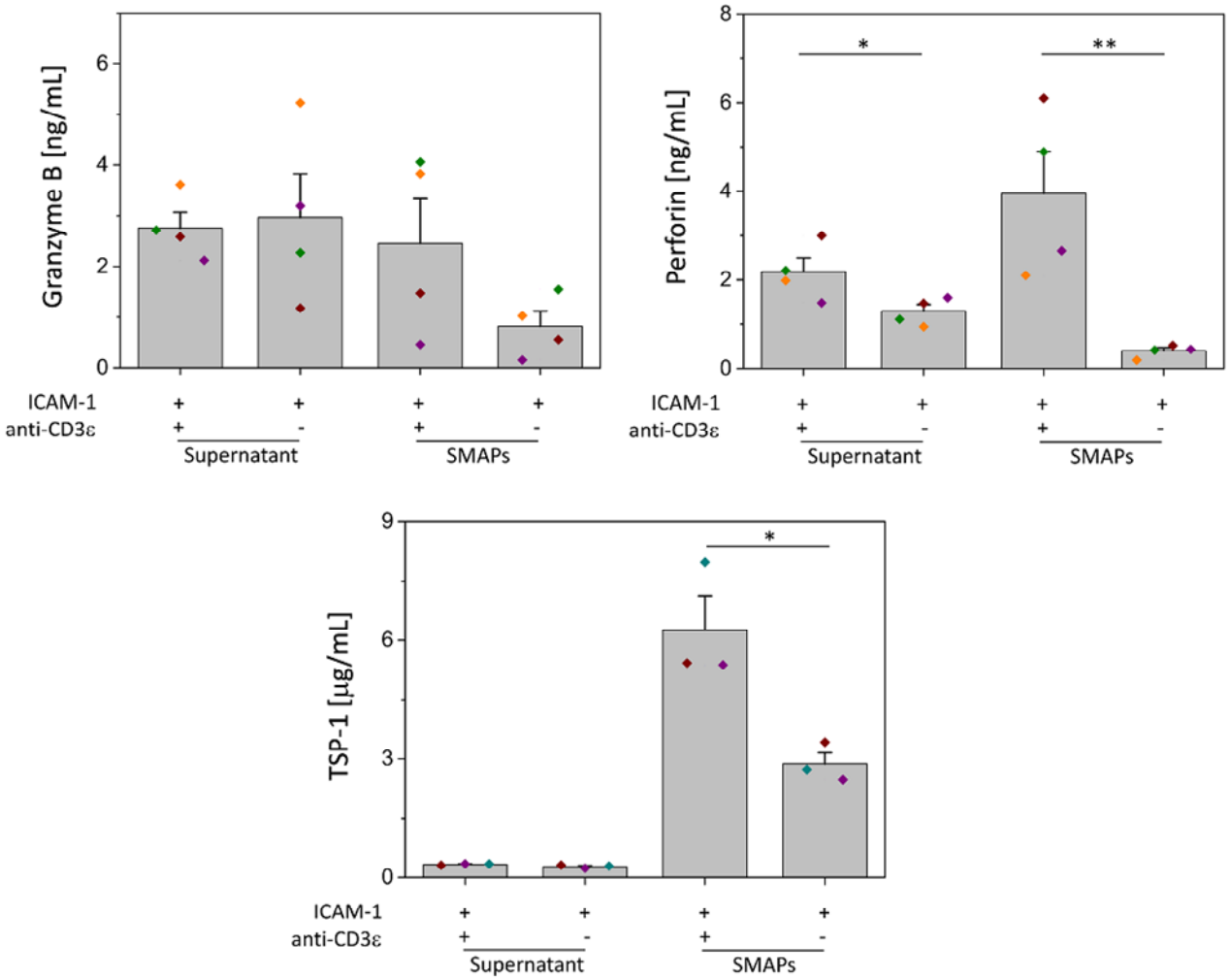

Fig. S12.

Detection of Gzmb, Prf1 and TSP-1 on CD8$^+$ T-cell released SMAPs by ELISA. SMAPs released on non-activating (ICAM-1) or activating (ICAM-1 + anti-CD3ε) SLB were lysed and analyzed by ELISA. Supernatants from non-activating and activating conditions were analyzed in parallel. Each colored dot represents one donor. Bars represent mean ± SEM. *, $p < 0.05$, **, $p < 0.01$. Not significant differences are not shown.

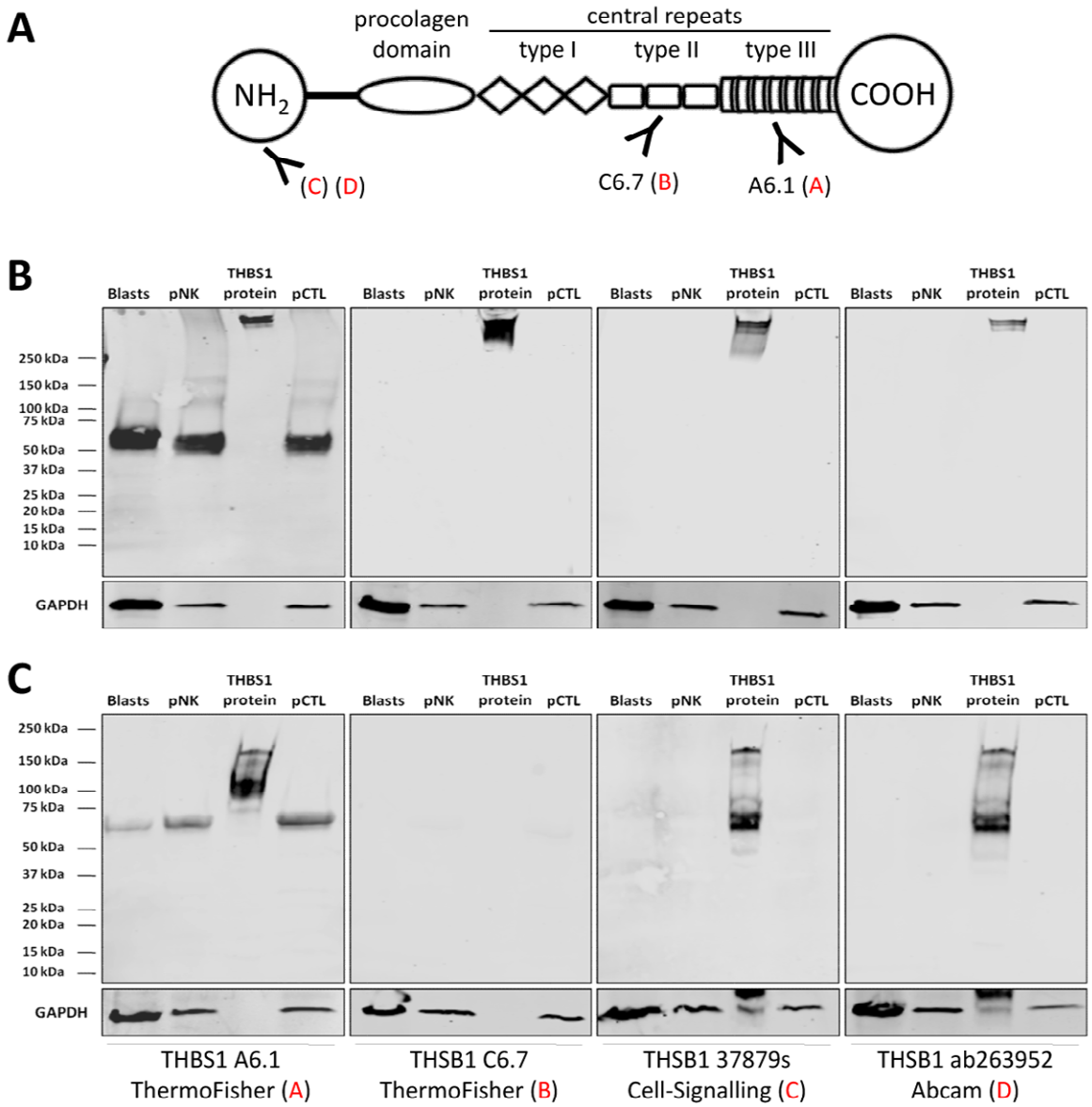

Fig. S13.

Detection of TSP-1 in CD8$^+$ T-cells and primary NK cells by immuno-blotting. (A) Schematic representation of epitopes placement along human TSP-1 protein. A to D marks the binding sites for the anti-TSP-1 antibodies used in this experiment. (B, C) Immuno-blotting analysis of TSP-1 in blasted CD8$^+$ T-cells (Blasts), primary NK cells (pNK) and primary CTLs (CD8$^+$ CD57$^+$ T-cells; pCTL) under non-reducing (B) and reducing (C) conditions with different anti-TSP-1

antibodies (as indicated below the panels). Purified full human TSP-1 protein isolated from platelets was used as a control. Note that the platelet material shows evidence of proteolysis to generate a 100 kDa C-terminal fragment and 60 kDa N-terminal fragment, but none of these match the C-terminal fragment found in CTLs and NK cells. Although we detected N-terminal peptides of TSP-1 in the mass spectrometry analysis (Fig S6C) these were not associated with immunoreactive domains in the SMAPs on SLB.

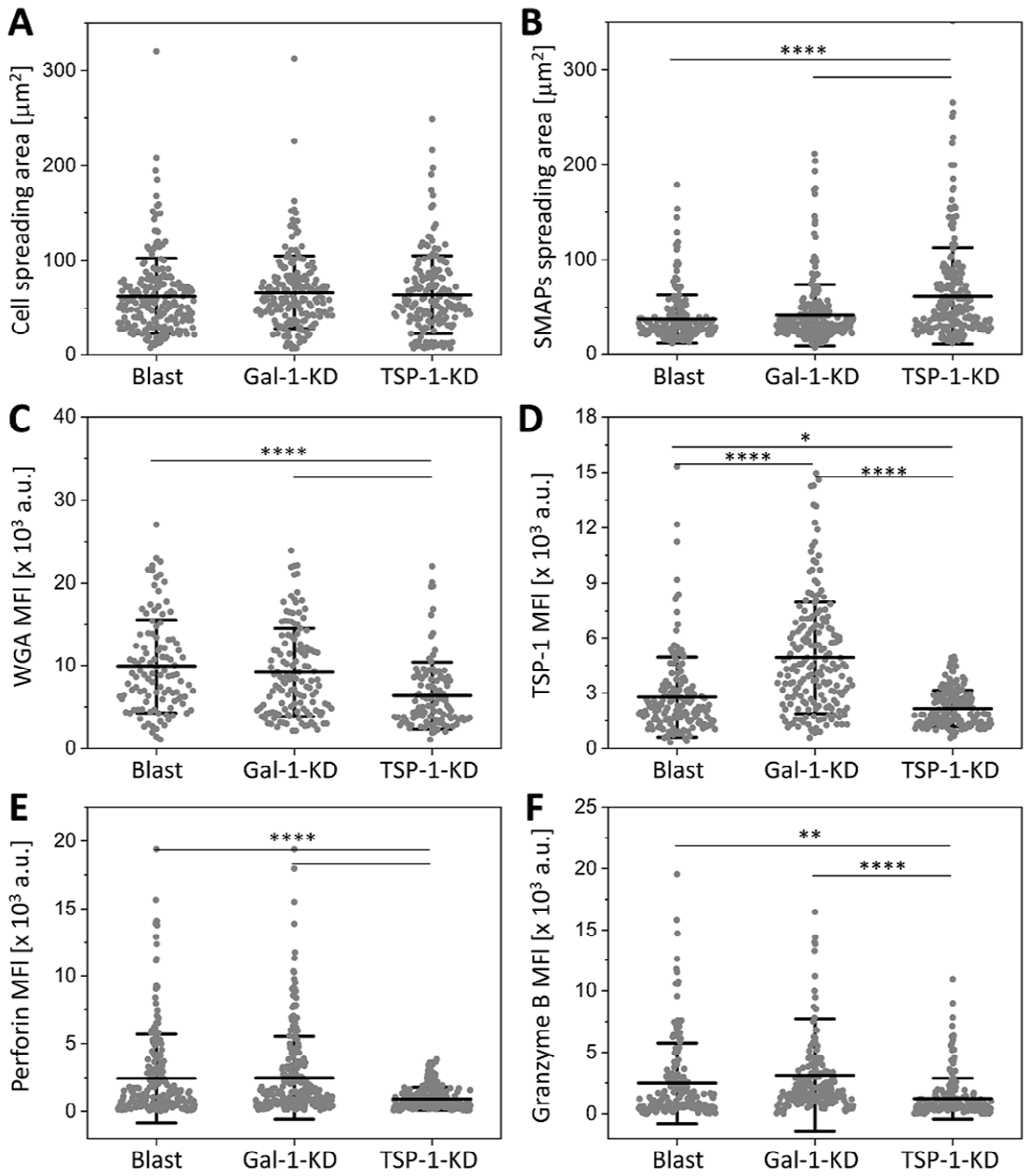

Fig. S14.

SMAPs released from TSP-1 knockout CD8⁺ T-cells contained less perforin and granzyme B. (A-B) CD8⁺ T-cell blasts (Blast), galectin-1 (Lgals1-CRISPR) and TSP-1 (TSP-1-CRISPR) genome edited CD8⁺ T-cell spreading area (A) and corresponding CD8⁺ T-cell released SMAPs spreading area (B) on activating SLB. (C-F) Mean fluorescent intensity (MFI) of WGA (C), TSP-

1 (D), Prf1 (E), and Gzmb (F) on released SMAPs. Each dot represents one cell (A) or the area occupied by the released SMAPs from one cell (B-F). Horizontal lines and error bars represent mean ± SD. *, $p < 0.05$, **, $p < 0.01$, ****, $p < 0.0001$. Not significant differences are not shown.

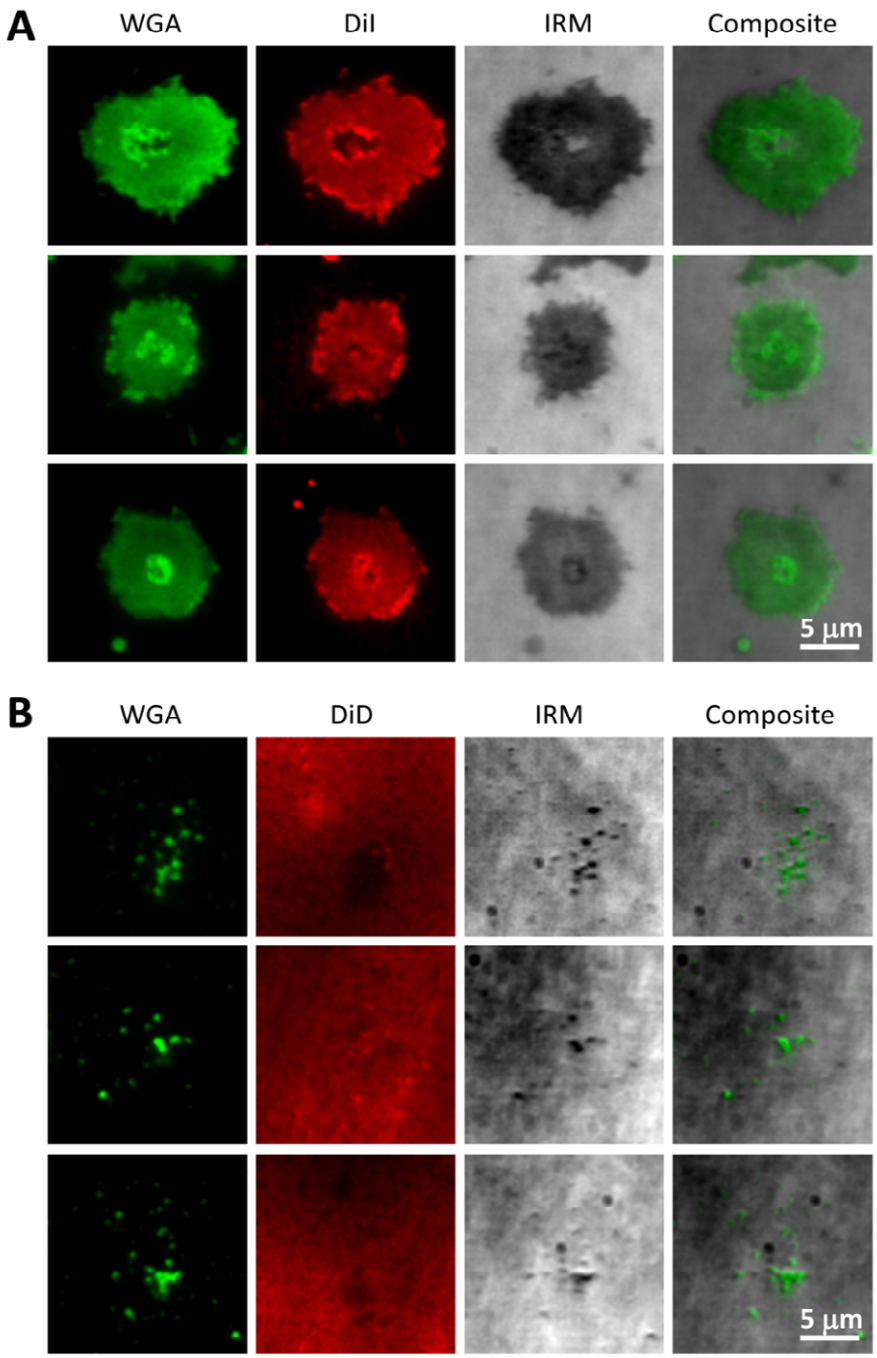

Fig. S15.

CD8$^+$ T-cells released SMAPs that contained glycoproteins but did not have a phospholipid membrane. Examples of TIRFM images of CD8$^+$ T-cells (A) and released SMAPs (B) captured on activating (ICAM-1 + anti-CD3ε) SLB labeled with WGA (green) or with a membrane dye

(DiI or DiD; red). Interference reflection microscopy (IRM) and composite images between WGA and IRM are shown. Scale bar, 5 μm.

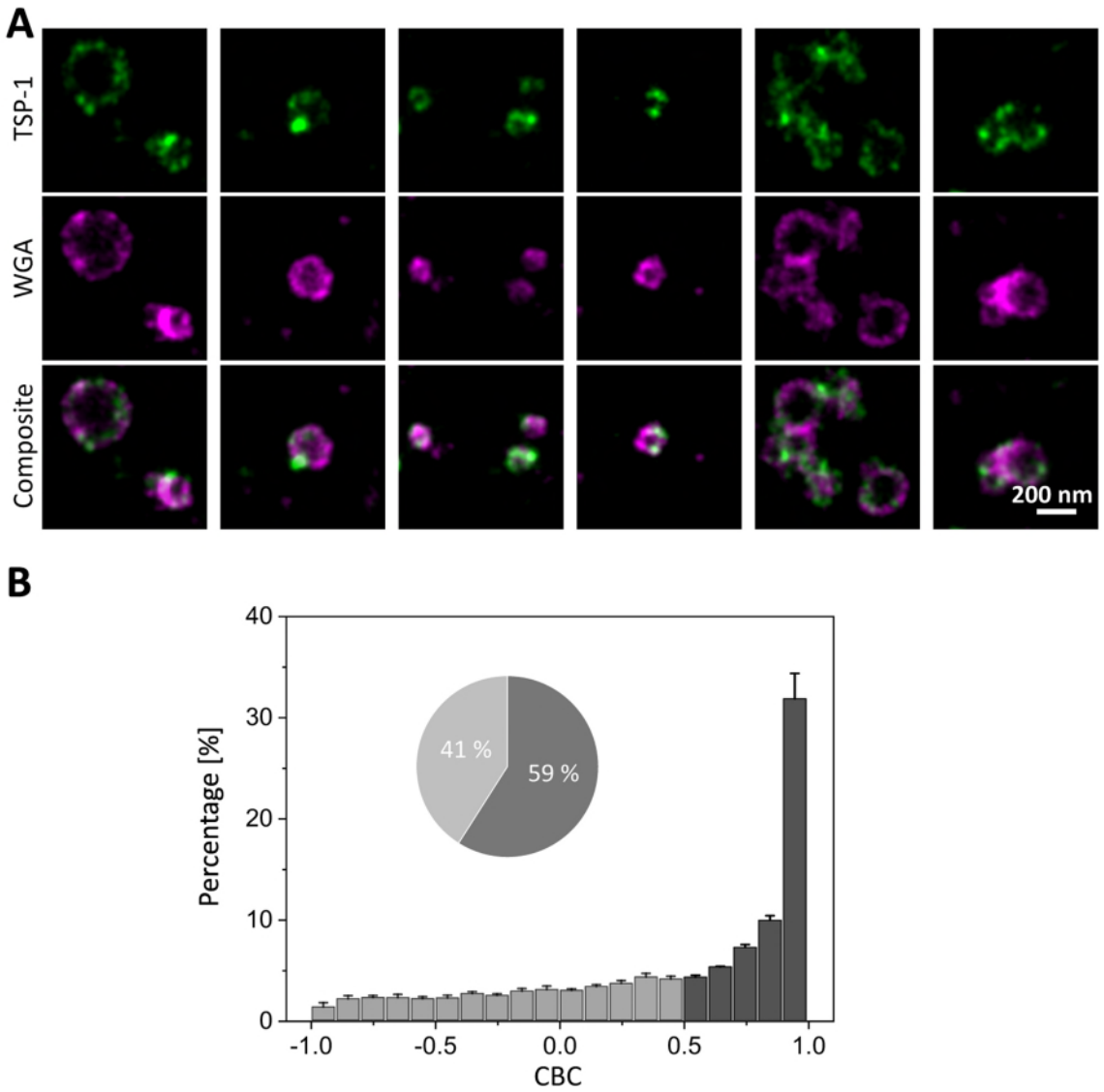

Fig. S16.

TSP-1 was a major constituent of SMAPs. (A) Examples of dSTORM images of individual SMAPs (labeled with WGA, magenta) positive for TSP-1 (green) released on activating (ICAM-1 + anti-CD3ε) SLB. Scale bar, 200 nm. (B) Quantification of the percentage of colocalization between TSP-1 and WGA staining assessed by Coordinate-Based Colocalization (CBC) analysis. Bars represent mean ± SD. The percentage of colocalization is the sum of percentages (59 ± 3 %) from +0.5 to +1 and is highlighted in dark grey.

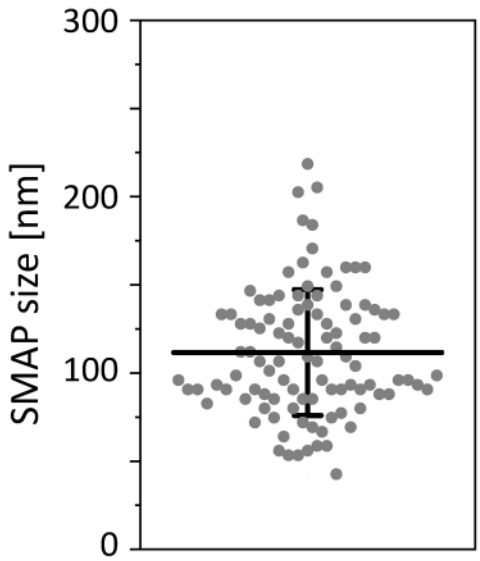

Fig. S17.

SMAPs sizes quantified from CSXT analysis. The average SMAP diameter was 111 ± 36 nm from n=101. Horizontal line and error bar represent mean ± SD.

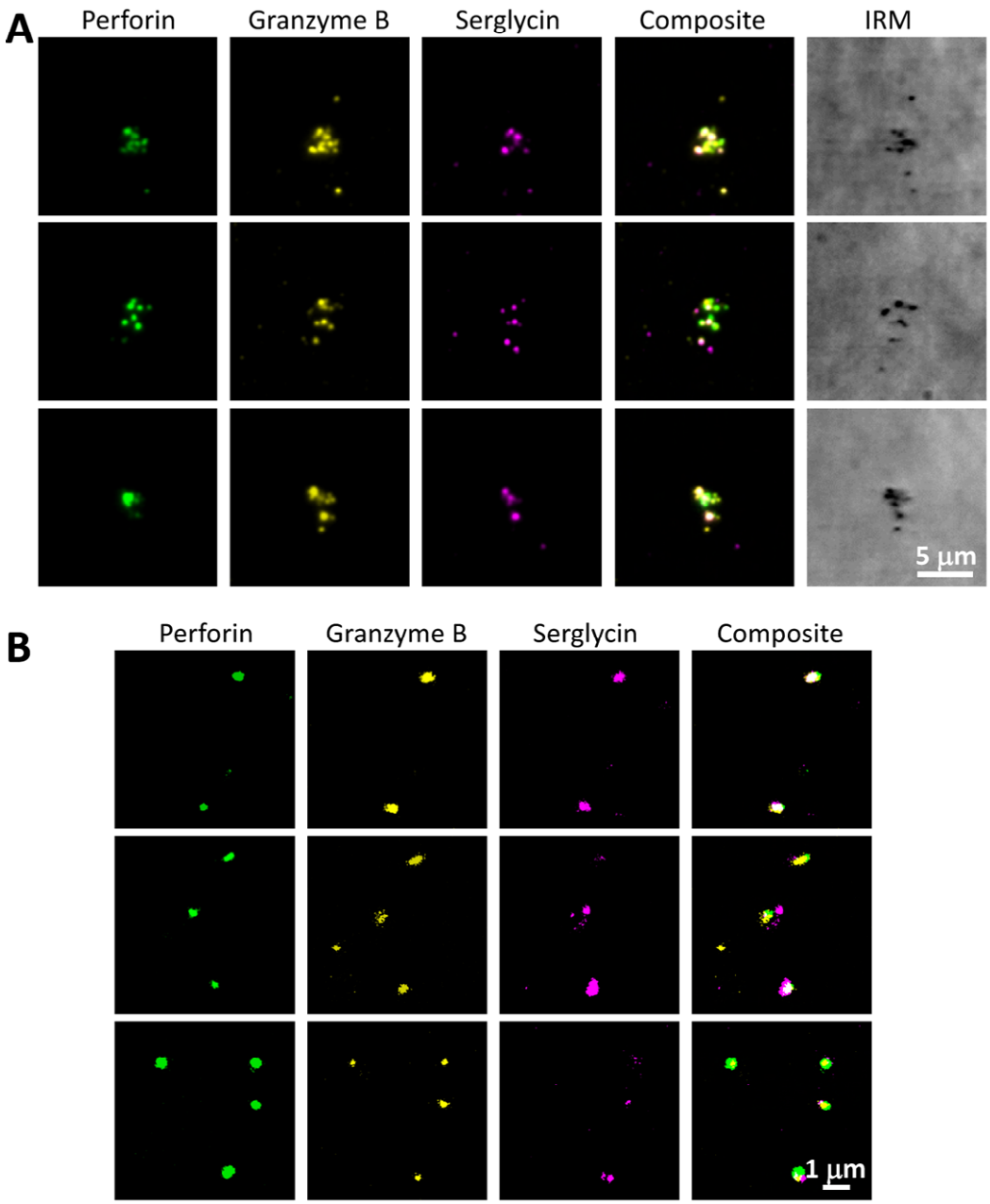

Fig. S18.

Srgn was a component of SMAPs. TIRFM (A) and dSTORM (B) images of CTL released SMAPs captured on activating SLB. SMAPs were labeled with anti-Prf1 (green), anti-Gzmb (yellow) and anti-Srgn (magenta) antibodies. Interference reflection microscopy (IRM) and composite images are shown. Three examples from different field of views are shown for each condition. Representative data from 2 experiments. Scale bar, 1 µm.

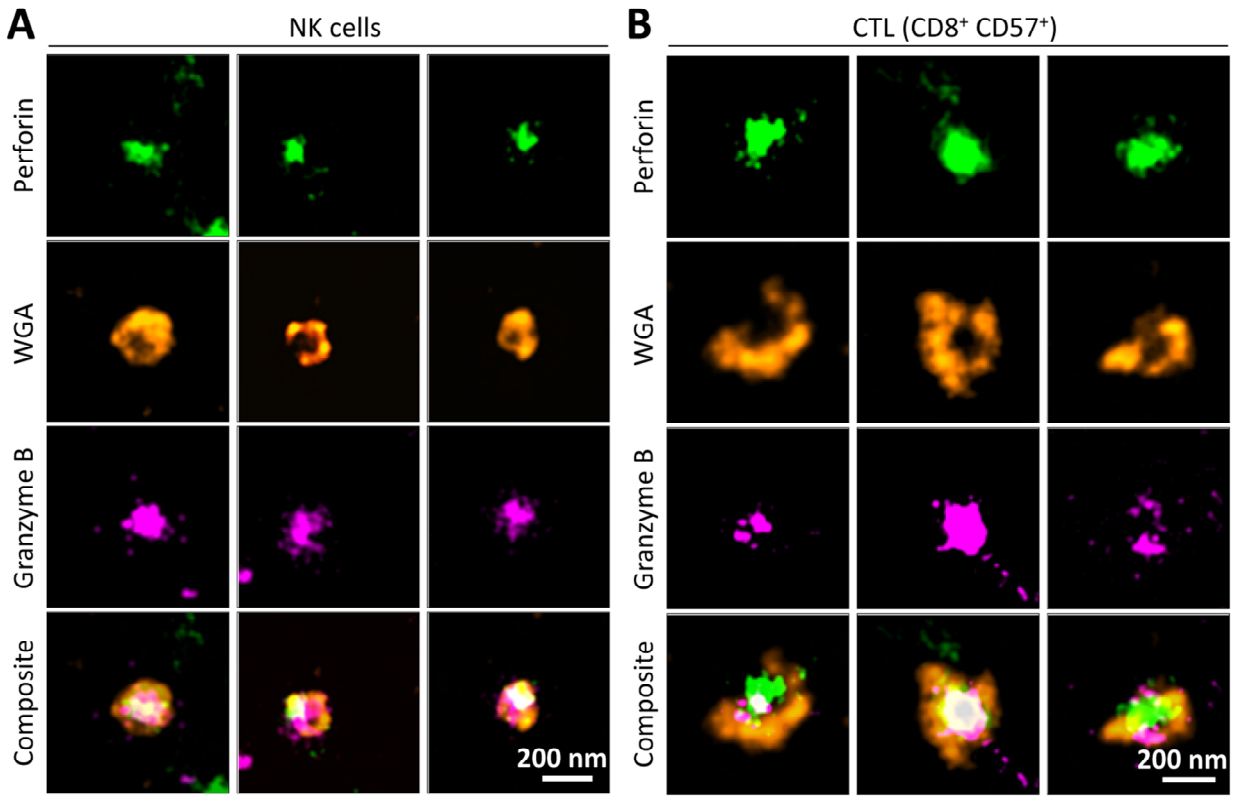

Fig. S19.

SMAPs released by primary NK and CTLs. dSTORM images of individual SMAPs positive for Prf1 (green), WGA (orange) and Gzmb (magenta) released by pNK cells (A) or primary CTLs (B). Scale bar, 200 nm.

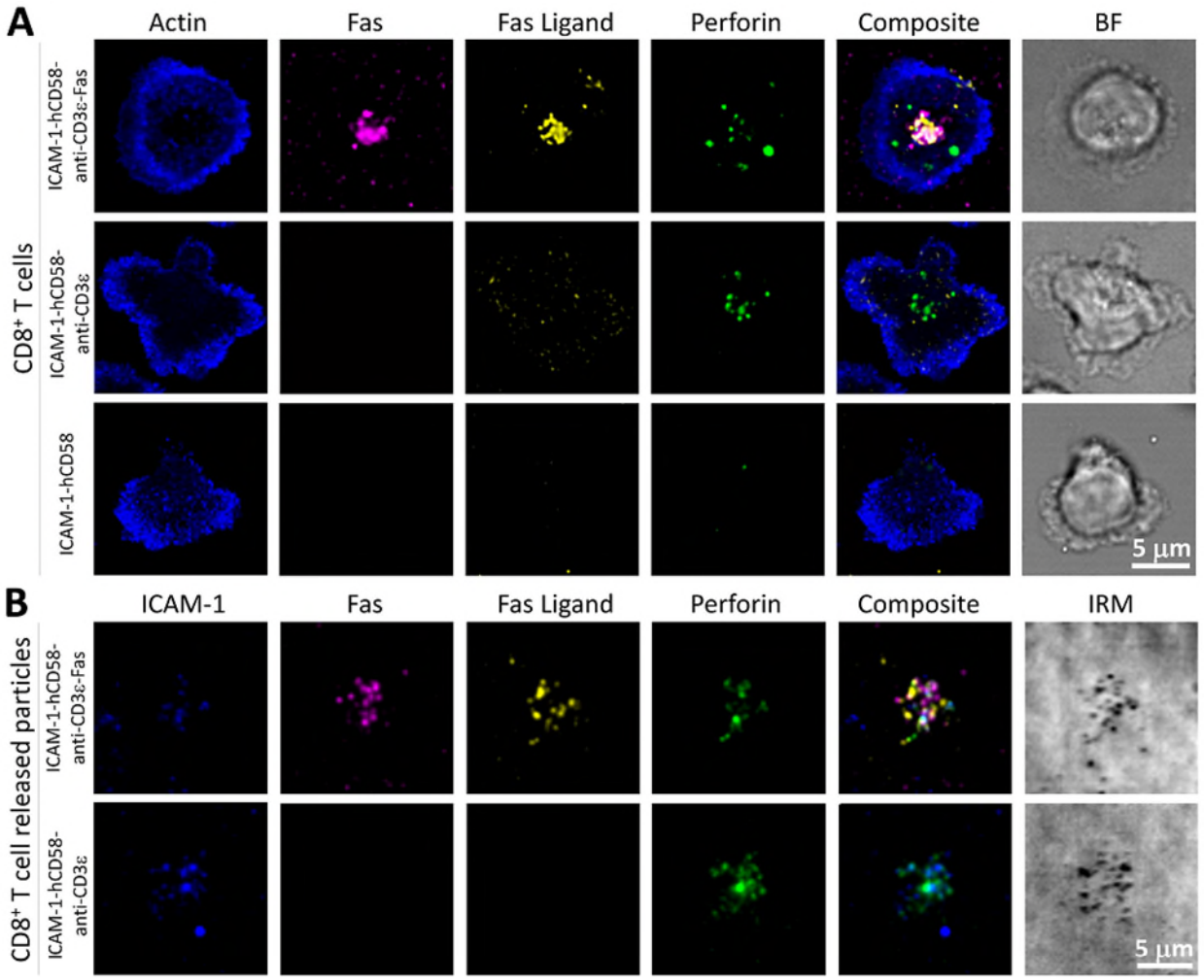

Fig. S20.

CTLs released particles containing FasL in response to Fas signal (A) Confocal images of CTLs captured on SLB loaded with hCD58 and ICAM-1 in the presence or absence of Fas-AlexaFluor647 (magenta) and anti-CD3ε (top panel). Cells were labeled with phalloidin to visualize actin (blue) and with anti-Fas Ligand (yellow) and anti-Prf1 (green) antibodies. Composite and bright field microscopy (BF) images are shown. (B) TIRFM images of CTL released particles captured on activating SLB (hCD58 + ICAM-1-AF405 (blue)) in the presence or absence of Fas-AlexaFluor647 (magenta). Particles were labeled with anti-Fas Ligand (yellow)

and anti-Prf1 (green) antibodies. Interference reflection microscopy (IRM) and composite images are shown. Scale bar, 5 μm.

Movie S1.

Live confocal imaging of the transfer of Gzmb-mCherry^{+} (green) and WGA (magenta) labeled SMAPs from an antigen specific CTL clone into pp65-pulsed JY target cells. BF, bright field microscopy. Frame rate, 3 frames/min.

Movie S2.

3D confocal *z*-stack projection depicting the transfer of Gzmb-mCherry^{+} (green) and WGA (magenta) labeled SMAPs from an antigen-specific CTL clone into pp65-pulsed JY target cells (cyan). BF, bright field microscopy.

Movie S3.

3D confocal *z*-stack projection depicting the absence of the transfer of Gzmb-mCherry^{+} (green) and WGA (magenta) labeled SMAPs from an antigen-specific CTL clone into unpulsed JY target cells (cyan). BF, bright field microscopy.

Movie S4.

Live TIRFM imaging of the release of SMAPs from Gzmb-mCherry-SEpHluorin (magenta/green) transfected CD8^{+} T-cells on activating (ICAM-1 (blue) + anti-CD3ε) SLB. Frame rate, 2 frames/min.

Movie S5.

Schematic of the working model for capturing SMAPs released by activated CD8^{+} T-cells. CD8^{+} T-cells (grey) were incubated on activating SLB for the desired time. After incubation, cells were removed with cold PBS leaving the released SMAPs (purple) on the SLB. Elements are not drawn to a scale.

Movie S6.

Live TIRFM imaging of the release of Prf1$^+$ (green) SMAPs by CD8$^+$ T-cells after contact with activating (ICAM-1 (blue) + anti-CD3ε) SLB. Frame rate, 1 frame/min.

Movie S7.

Live TIRFM imaging of the release of Gzmb$^+$ (red) SMAPs by CD8$^+$ T-cells after contact with activating (ICAM-1 (blue) + anti-CD3ε) SLB. Frame rate, 1 frame/min.

Movie S8.

Live TIRFM imaging of the release of SMAPs double positive for Prf1 (green) and Gzmb (magenta) by CD8$^+$ T-cells after contact with activating (ICAM-1 (blue) + anti-CD3ε) SLB. Frame rate, 1 frame/min.

Movie S9.

Live TIRFM imaging of the release of SMAPs double positive for Prf1 (green) and Gzmb (magenta) by CD8$^+$ T-cells after contact with activating (ICAM-1 (blue) + anti-CD3ε) SLB. Frame rate, 1 frame/min.

Movie S10.

Live TIRFM imaging of the release of Prf1$^+$ (green) and TSP-1$^+$ (magenta) SMAPs by CD8$^+$ T-cells after contact with activating (ICAM-1 (blue) + anti-CD3ε) SLB. Frame rate, 1 frame/min.

Movie S11.

3D confocal *z*-stack projection and orthogonal views of CD8$^+$ T cells co-transfected with Gzmb-mCherry-SEpHluorin (magenta) and TSP-1-GFPSpark (green) on non-activating (ICAM-1; left)

or activating (ICAM-1 + anti-CD3ε; right) SLB. Cells were stained with WGA (yellow) to visualize the cell membrane. The formation of a mature IS is indicated by an ICAM-1 ring (blue).

Movie S12.

CSXT projection and 3D reconstruction of individual released SMAPs captured on a carbon coated EM grid containing ICAM-1 and anti-CD3ε.

Movie S13.

CSXT projection and 3D reconstruction of a $CD8^+$ T-cell interacting with a carbon coated EM grid containing ICAM-1 and anti-CD3ε. SMAPs can be observed within the multivesicular bodies inside the cell.

Movie S14.

CSXT projection and 3D reconstruction of a $CD8^+$ T-cell interacting with a carbon coated EM grid containing ICAM-1 and anti-CD3ε. Released SMAPs (yellow) can be observed beneath the cell. Nucleus is highlighted in blue.

Data S1.

List of proteins present in $CD8^+$ T-cell released SMAPs identified by mass spectrometry. Unfiltered list of proteins present in $CD8^+$ T-cell released SMAPs under activating (ICAM-1 + anti-CD3ε; light blue) or non-activating (ICAM-1; light green) conditions, identified by mass spectrometry (n=3 donors).